Hepatitis C virus kinetics by administration of pegylated interferon- α in human and chimeric mice carrying human hepatocytes with variants of the *IL28B* gene

Tsunamasa Watanabe, Fuminaka Sugauchi, Yasuhito Tanaka, et al.

Gut published online November 7, 2012
doi: 10.1136/gutjnl-2012-302553

Notes

Journal of Medical Virology 84:587–595 (2012)

Multiple Intra-Familial Transmission Patterns of Hepatitis B Virus Genotype D in North-Eastern Egypt

Mostafa Ragheb,[1] Abeer Elkady,[2] Yasuhito Tanaka,[2]* Shuko Murakami,[2] Fadia M. Attia,[3] Adel A. Hassan,[1] Mohamed F. Hassan,[1] Mahmoud M. Shedid,[1] Hassan B. Abdel Reheem,[1] Anis Khan,[2] and Masashi Mizokami[4]

[1]*Department of Endemic and Infectious Disease, Suez Canal University, Ismailia, Egypt*
[2]*Department of Virology and Liver Unit, Nagoya City University Graduate School of Medical Sciences, Kawasumi, Mizuho, Nagoya, Japan*
[3]*Department of Clinical Pathology Faculty of Medicine, Suez Canal University, Ismailia, Egypt*
[4]*Research Centre for Hepatitis and Immunology, International Medical Centre of Japan Konodai Hospital, Tokyo, Japan*

The transmission rate of intra-familial hepatitis B virus (HBV) and mode of transmission were investigated in north eastern Egypt. HBV infection was investigated serologically and confirmed by molecular evolutionary analysis in family members (N = 230) of 55 chronic hepatitis B carriers (index cases). Hepatitis B surface antigen (HBsAg) and hepatitis B core antibody (anti-HBc) prevalence was 12.2% and 23% among family members, respectively. HBsAg carriers were prevalent in the age groups; <10 (16.2%) and 21–30 years (23.3%). The prevalence of HBsAg was significantly higher in the family members of females (19.2%) than males (8.6%) index cases ($P = 0.031$). HBsAg and anti-HBc seropositive rates were higher significantly in the offspring of females (23%, 29.8%) than those of the males index cases (4.3%, 9.8%) ($P = 0.001$, 0.003), as well as higher in the offspring of an infected mother (26.5, 31.8%) than those of an infected father (4.7%, 10.5%) ($P = 0.0006$, 0.009). No significant difference was found in HBsAg seropositive rates between vaccinated (10.6%) and unvaccinated family members (14.8%). Phylogenetic analysis of the preS2 and S regions of HBV genome showed that the HBV isolates were of subgenotype D1 in nine index cases and 14 family members. HBV familial transmission was confirmed in five of six families with three transmission patterns; maternal, paternal, and sexual. It is concluded that multiple intra-familial transmission routes of HBV genotype D were determined; including maternal, paternal and horizontal. Universal HBV vaccination should be modified by including the first dose at birth with (HBIG) administration to the newborn of mothers infected with HBV. *J. Med. Virol. 84:587–595, 2012.* © 2012 Wiley Periodicals, Inc.

KEY WORDS: HBV genotype D; intra-familial transmission; vaccine

INTRODUCTION

Chronic hepatitis B virus (HBV) infection is a major health problem worldwide and is affecting approximately 350 million individuals [Lee, 1997]. Infection with HBV may lead to chronic state of hepatitis in 5–10% of patients who acquired the infection in the adult life and in 80–90% of patients who acquired the infection in the infancy [Chen, 1993]. Infection with HBV can lead to a progressive liver disease including liver cirrhosis and hepatocellular carcinoma (HCC) with approximately 1 million HBV-associated deaths from HCC every year [Seeger and Mason, 2000; Kao and Chen, 2002].

Based on the proportion of the population who are seropositive for hepatitis B surface antigen (HBsAg),

Grant sponsor: The Grant for National Center For Global Health and Medicine; Grant number: 22A-9; Grant sponsor: Grant-in-Aid for Japan Society for the Promotion of Science (JSPS) Fellows; Grant number: 21.09355.

Mostafa Ragheb and Abeer Elkady contributed equally to this study.

*Correspondence to: Yasuhito Tanaka, MD, PhD, Department of Virology and Liver Unit, Nagoya City University Graduate School of Medical Sciences, Kawasumi 1, Mizuho, Nagoya 467-8601, Japan. E-mail: ytanaka@med.nagoya-cu.ac.jp

Accepted 19 December 2011

DOI 10.1002/jmv.23234
Published online in Wiley Online Library (wileyonlinelibrary.com).

the world is divided conceptually into zones of high, intermediate, and low HBV endemic areas [Lavanchy, 2004]. In countries where the HBV infection is endemic, most infections result from the vertical transmission from the mother to the child in the peripartum period or from the infection in the early childhood. In the low HBV endemic regions, the neonatal or the childhood HBV infection is rare or even sporadic and the transmission of HBV occurs primarily among unvaccinated adults through the sexual transmission and injecting drug use [Custer et al., 2004].

Patients with chronic hepatitis B are considered to be the major reservoirs for the transmission of HBV. High incidence of infection with HBV is observed within the household contacts of chronic HBV carriers and it is not rare to have several members of the same household who have evidence of infection with HBV [Milas et al., 2000; Thakur et al., 2002]. However, the precise mechanisms of intra-familial spread have not been established clearly.

Different prophylactic strategies for controlling the HBV infection have been used by different countries depending on the prevalence of the HBV infection in each country [Poland and Jacobson, 2004]. The widespread immunization program against hepatitis B, which was implemented in more than 100 countries, was capable of dramatic reduction in the occurrence of chronic HBV infection and HCC [Zuckerman, 1997]. In Egypt, the HBV vaccine was included in 1992 in the Expanded Program of Immunization with injection at 2, 4, and 6 months of age [El Sherbini et al., 2006]. This program resulted in a significant reduction in the rate of acute symptomatic hepatitis B among the children in the age group eligible to receive the vaccine [Zakaria et al., 2007].

At least eight HBV genotypes have been identified based on the divergence of 8% or more of the entire nucleotide sequence and most of the HBV genotypes have a distinct geographical distribution [Okamoto et al., 1988; Norder et al., 1994; Stuyver et al., 2000]. Accumulated evidences indicated the difference in the virological characteristics among different HBV genotypes, which is reflected by the difference in the clinical outcome of infection with hepatitis B according to the infecting genotype [Miyakawa and Mizokami, 2003; Schaefer, 2005; Ozasa et al., 2006; Sugiyama et al., 2006]. However, data regarding the specificity of the transmission routes of each genotype is still scarce globally and need to be clarified.

The prevalence of HBV ranges between 2% and 6% in Egypt with the predominance of infection with HBV genotype D [Zekri et al., 2007]. It is widely known that Egypt is one of the countries with highest prevalence rate of infection with HCV in the world [el-Zayadi et al., 1992; Arthur et al., 1993; el Gohary et al., 1995]. However, the burden of HBV related progressive liver disease including liver cirrhosis and HCC in Egypt is observable either single or in a dual infection with HCV [Abdel-Wahab et al., 2000; el-Zayadi et al., 2005].

This study aimed to evaluate the prevalence of infection with HBV within the families of chronic HBV carriers in north Eastern Egypt. In addition, the intra-familial mode of transmission of HBV genotype D was also examined in the current cohort by the molecular evolutionary analyses. The impact of the HBV immunization programme in protecting this high-risk group was also investigated.

PATIENTS AND METHODS

Patients

The present study was conducted between January 2008 and June 2008 at the Communicable Disease Research and Training Centre, in Suez city. The study protocol was approved by the ethics committees of the participating institution and an informed consent was obtained from the included subjects.

Chronic HBV carriers were defined as individuals whose serum samples tested positive for HBsAg for at least 6-months period. Patients who fulfilled the criteria of chronic HBV carriers and were first detected within their families, were defined as the index cases ($n = 55$). The index cases included 40 (72.7%) men and 15 (27.3%) women. Their mean age ($\pm$ SD) was 41 ± 10.7 years and all the index cases were negative for HBeAg.

A total of 230 household contacts of the index cases were included in the study and defined as family members group. Data regarding their family relationship to the index cases, age, and the HBV vaccination history have been obtained.

According to the kinship of the family members to the index case group, the family members included 139 offspring, 4 parents, 46 spouses, 15 siblings, and 26 defined as other relatives who are living in the same house with the index cases.

Serological Methods

Serum samples were collected from the index cases and family members groups.

The Serum samples were examined for HBsAg, anti-HBc, anti-HBs, and HBeAg by the chemiluminescence enzyme immunoassay with the commercial assay kits (Fujirebio, Inc., Tokyo, Japan). The examination of the serum samples for anti-HCV and HIV was conducted using commercial kits (Abbott Laboratories, Abbott Park, IL).

Molecular Evolutionary Analysis

The HBV/DNA was extracted from 200 μl of serum samples positive for HBsAg using the QIAamp DNA MiniKit (QIGEN, Inc., Hilden, Germany), and re-suspended in 100 μl of a storage buffer (provided by the kit manufacturer).

The entire preS2 and S regions of the HBV genome (799 nucleotides; nucleotide positions 34–833) were amplified using the primers set and the conditions described previously [Sugauchi et al., 2001].

The amplified products were sequenced using Prism Big Dye (Pekrin–Elmer Applied Biosystems, Foster City, CA) in the ABI 3100 DNA automated sequencer according to the manufacturer's protocol. The sequences were aligned together with the CLUSAL X software programme [Thompson et al., 1994].

The phylogenetic tree was constructed using the neighbor joining method with Tamura-Nei's distance correction model using the Online Hepatitis Virus database (http://s2as02.genes.nig.ac.jp/) [Shin et al., 2008]. The Bootstrap values were determined on 1000 database resampling tests. The sequences of other HBV isolates used for the construction of the phylogenetic tree were retrieved from the DDBJ/EMBL/GenBank sequence database and were indicated in their accession numbers. The new nucleotide sequences data that were reported in this manuscript will appear in the DDBJ/EMBL/GenBank sequence database with accession numbers AB561825-AB561856.

Statistical Analysis

Statistical analysis was performed with the Fisher's exact probability test and the independent *t*-test for the continuous variables using the SPSS software package (SPSS, Chicago, IL). *P*-values (two-tailed) <0.05 were considered to be significant statistically.

RESULTS

The family member included 96 (41.7%) males and 134 females (58.3%). Their mean age (±SD) was 20.6 ± 14.6. The rate of seropositivity for HBsAg and anti-HBc was 12.2% (28/230) and 23% (53/230) of the family members group with no statistical significant difference between the males and females members.

Age Group Distribution of HBV Infection Within the Family Members Group

Figure 1 illustrates the HBsAg and anti-HBc prevalences among different age groups of the family members. The highest prevalence of HBsAg seropositive cases was observed in the age group, 21–30 years old; (10/43; 23.3%) followed by the age group, 0–10 years old; (11/68; 16.2%). No statistical significant difference was found in the HBsAg seropositive rates between these two age groups. The prevalence of HBsAg was 7.7% (5/65), 3.4% (1/29), and 4% (1/25) in the age groups; 11–20, 31–40, and ≥41 years old, respectively. The prevalence of anti-HBc seropositive cases was significantly increasing with the age and the highest rate was observed in the age group ≥41 years old. The prevalence of anti-HBc was 8.8% (6/68), 20% (13/65), 25.6% (11/43), 37.9% (11/29), and 48% (12/25) in the age groups; 0–10, 11–20, 21–30, 31–40, and ≥41 years old, respectively.

The HBsAg and anti-HBc seropositive rates were analyzed in the family members with respect to their relationship to the index cases (Fig. 2A). As overall, the HBsAg was positive in 6.5% (3/46) spouse of index cases, 10.8% (15/139) of the offspring, 25% (1/4) of the parents, and 40% (6/15) of the siblings (Fig. 2A).

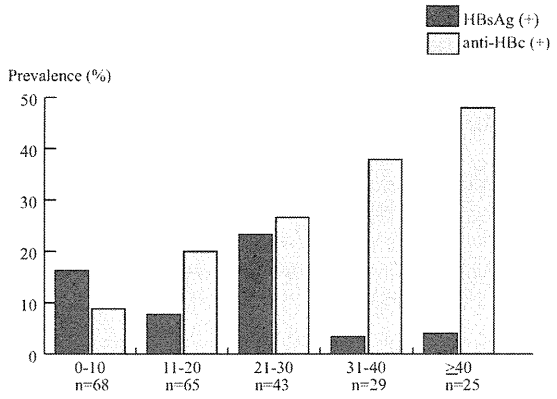

Fig. 1. Age distribution and HBV serological status among family members.

The prevalence of anti-HBc was 34.8% (16/46) in the spouse of index cases, 17.3% (24/139) in the offspring, 50% (2/4) in the parents, and 46.7% (7/15) in the siblings of the index cases (Fig. 2A).

Interestingly, the prevalence of HBsAg and anti-HBc was significantly higher in the family members of the females (19.2%, 15/78) than that of the males index cases (8.6%, 13/152; $P = 0.034$) and a trend of higher incidence of anti-HBc in the family members of the females than the males index cases (Fig. 2B). Among the offspring group, HBsAg and anti-HBc seropositive rates were significantly higher in the offspring of the females index cases (HBsAg; 23%, 11/47, anti-HBc; 29.8%, 14/47) cases than in the offspring of the males index cases (HBsAg; 4.3%, 4/92, antiHBc; 9.8%, 9/92), ($P = 0.001$, 0.003 respectively; Fig. 2C).

Further analysis was performed regarding the HBsAg seropositive rate in the offspring according to HBV infection of both one and two parents and the parent gender who is infected with HBV. Significantly higher rate of HBsAg positive (26.5%, 13/49) and anti-HBc positive (31.8%, 14/49) off spring were found in families where the mother was positive for HBsAg compared with families where the father was HBsAg positive (HBsAg; 4.7%, anti-HBc; 10.5%), ($P = 0.0006$, 0.009 respectively) (data not shown).

The seropositive rate of HBsAg was higher in the non-sexual contacts (13.6%, 25/184) of the index cases (parents, offspring, siblings, and cousins) than the sexual contacts (spouses; 6.5%, 3/46) with no statistical significant difference. Anti-HBc seropositive cases were observed more frequently in the sexual contacts (spouses) than in the non-sexual contacts (parents, offspring, siblings cousins) of the index cases. (Sexual vs. non-sexual contacts, 34.8% vs. 20.1%, $P = 0.049$) (data not shown).

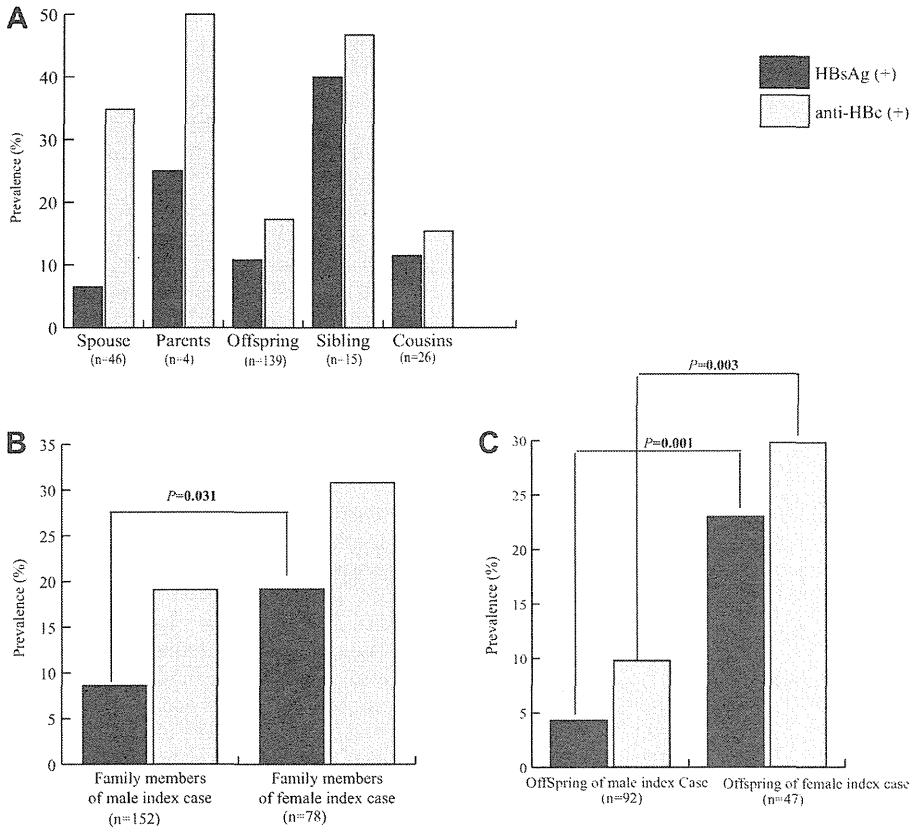

Fig. 2. Prevalence of HBsAg and anti-HBc within family members stratified by relationship to the index cases (**A**). HBV serological status of family members according to gender of the index case (**B**), and HBV serological status of the offspring according to HBV infected parent (**C**).

Molecular Evolutionary Analysis and Transmission Pattern of Hepatitis B in the Family Members Group

Eighteen index cases out of 55 (32.7%) were found to have at least one family member positive for HBsAg. The age range of these index cases was 26–56 years and 50% (9/18) of them were male (Table I). Twenty-eight family members were found to be positive for HBsAg. The data regarding the degree of relativity of each family member infected with HBV to the index case, the age of the infected family member, and the vaccination status were indicated in Table I. The mean age (±SD) of the family members with active HBV infection was 17.8 ± 13.0 years old (Table I).

The HBV genomic region of 799-nt length and spanning PreS2 and S region was amplified in 44% (8/18) of the index cases and in 50% (14/28) of the family members infected with HBV. However, the target genomic region could be amplified and sequenced simultaneously in the index cases and their related family members in six subjects. These six subjects are defined in the present report, Table I and Figure 3 as F 3, F4, F19, F35, F37, and F 43 (Table I, Fig. 3).

To confirm the family clustering, a phylogentic tree was constructed by (1) the previous mentioned sequences (2) sequences isolated from the index cases whose family members were negative for HBsAg (3) HBV nucleotide sequences isolated from HBV chronic carriers residing in different districts in Egypt (North and South) either retrieved from the data base band or further included in the present study.

The phylogenetic analysis of the preS2 and S regions of the HBV genome revealed that the HBV isolates were of subgenotype D1 (Fig. 3). Using the phylogenetic analysis, in family 4 (F4), a high homology was detected between the HBV strains isolated from the grandmother together with her daughters and her grandchildren (Fig. 3). In the Family 35 and Family 43 (F35, and F43), the father and the child harbored very closely related HBV isolates and the phylogenetic analysis suggesting that the father may have been the source of infection for his child in Family 35 (F35) and Family 43 (F43). Similarly, very closely related HBV isolates were also detected in the

TABLE I. Descriptive Analysis of the Family Members Positive for the HbsAg

Subject	Relation (gender)	Age	HBV-vaccine[a]	PreS2 + S
F3	Index (F)	42		(+)
F3-1[b]	Daughter	13	Yes	(+)
F10	Index (F)	30		(−)
F10-1	Daughter	3	Yes	(+)
F11	Index (F)	33		(+)
F11-1	Daughter	8	Yes	(−)
F11-2	Cousin	10	Yes	(−)
F30	Index (F)	42		(−)
F30-1	Son	8	Yes	(−)
F34	Index (F)	30		(−)
F34-1	Son	7	Yes	(+)
F34-2	Son	9	Yes	(+)
F48	Index (F)	30		(−)
F48-1	Son	5	Yes	(−)
F35	Index (M)	29		(+)
F35-1[b]	Daughter	5	Yes	(+)
F39	Index (M)	33		(−)
F39-1	Daughter	5	Yes	(−)
F43	Index (M)	47		(+)
F43-1[b]	Daughter	12	Yes	(+)
F55	Index (M)	56		(+)
F55-1	Daughter	12	Yes	(−)
F37	Index (M)	45		(+)
F37-1[b]	Wife	26	Yes	(+)
F36	Index (M)	31		(−)
F36-1	Brother	26	No	(−)
F36-2	Brother	28	No	(−)
F36-3	Brother	22	No	(+)
F36-4	Mother	63	No	(+)
F4	Index (F)	54		(+)
F4-1	Daughter	35	No	(+)
F4-2	Daughter	20	No	(+)
F4-3	Grandchild	6	Yes	(+)
F4-4[b]	Grandchild	4	Yes	(+)
F19	Index (M)	29		(+)
F19-1[b]	Wife	27	No	(+)
F40	Index (M)	26		(−)
F40-1	Relative	24	No	(−)
F40-2	Relative	29	No	(−)
F41	Index (F)	53		(−)
F41-1	Daughter	23	No	(−)
F41-2	Daughter	17	No	(−)
F45	Index (M)	33		(+)
F45-1	Wife	27	No	(−)
F50	Index(F)	27		(−)
F50-1	Sister	25	No	(−)

[a]HBV vaccination history is provided for the family member.
[b]Index and family members who are positive simultaneously for the PreS2and S region.

man and his wife in Families 19 and 37 (F19 and F37) (Fig. 3). The molecular evolutionary analysis of the sequences isolated from the mother and her daughter in Family 3 (F3), yielded two separate but distinct groupings of the HBV isolates, suggesting that the presence of two different HBV viral isolates infecting the mother and her daughter (Fig. 3).

Serological Markers of HBV Infection in the Vaccinated and Unvaccinated Family Members

The family members group was subdivided into two subgroups according to the history of full regimen schedule of HBV vaccination as shown in Table II; (1) A group of vaccinated family members which includes a total of 142 subjects, who received the complete HBV vaccine regimen. (2) A group of unvaccinated family members, which included 88 subjects with no previous history or incomplete regimen of HBV vaccination.

The family members in the unvaccinated group were significantly older (mean ± SD; 32.5 ± 12.5 years old) than in the vaccinated group (mean ± SD; 13.3 ± 10.4, $P = 0.012$). No statistical significant difference was found in the male gender distribution between the two groups. The anti-HBs seropositive rate was significantly higher in the vaccinated group than the unvaccinated group [69.8% (99/142) vs. 33% (29/88), respectively, $P < 0.0001$] (Table II). The mean anti-HBs titre was significantly higher in the vaccinated than unvaccinated family members (70.1 ± 129.7 vs. 21.6 ± 51.7 mIU/ml, respectively $P < 0.0001$).

The prevalence of anti-HBc was significantly higher in the unvaccinated family members compared to vaccinated groups (37.5% vs. 14.1% respectively, $P < 0.0001$). Interestingly, no statistical significant difference was detected between the vaccinated and the unvaccinated groups regarding the prevalence of HBsAg [vaccinated vs. unvaccinated; 10.6% (15/142) vs. 14.8% (13/88), $P = 0.4$] (Table II). The HBV DNA was detected in 50% of family members positive for HBsAg with no statistical significant difference between the vaccinated (53%, 8/142) and unvaccinated groups (46.2%, 6/88) (Table II).

Mutations in the "a" determinant region. The available nucleotide sequences spanning the S gene of HBV isolated from the nine vaccinated and five unvaccinated members were translated into amino acid and aligned in correspondence to the reference sequences. The amino acid substitutions in the "a" determinant region that was reported to be associated with vaccine escape mutation were not detected. However, an amino acid substitution at the second loop of "a" determinant region (T143L) was clustered in the family subject F37 (F37 and F37-1) and found in one unvaccinated family member (F4-1). Another substitution was detected in the second loop of "a" determinant region (T140I) in an unvaccinated member (F36-1). P127A substitution in first loop of the "a" determinant region was clustered in the family 43(F43 and F43-1; Fig. 4).

DISCUSSION

The investigation of the intra-familial transmission in a particular region usually reveals valuable information about the routes of HBV spread in general and may help in exploring the HBV spread problem and local peculiarities. This study is the first one in Egypt done to explore the intra-familial spread of HBV infection and inclusively HBV genotype D transmission routes in Egypt. An evaluation of the impact of the universal HBV vaccination on the intra-familial transmission of HBV was also done.

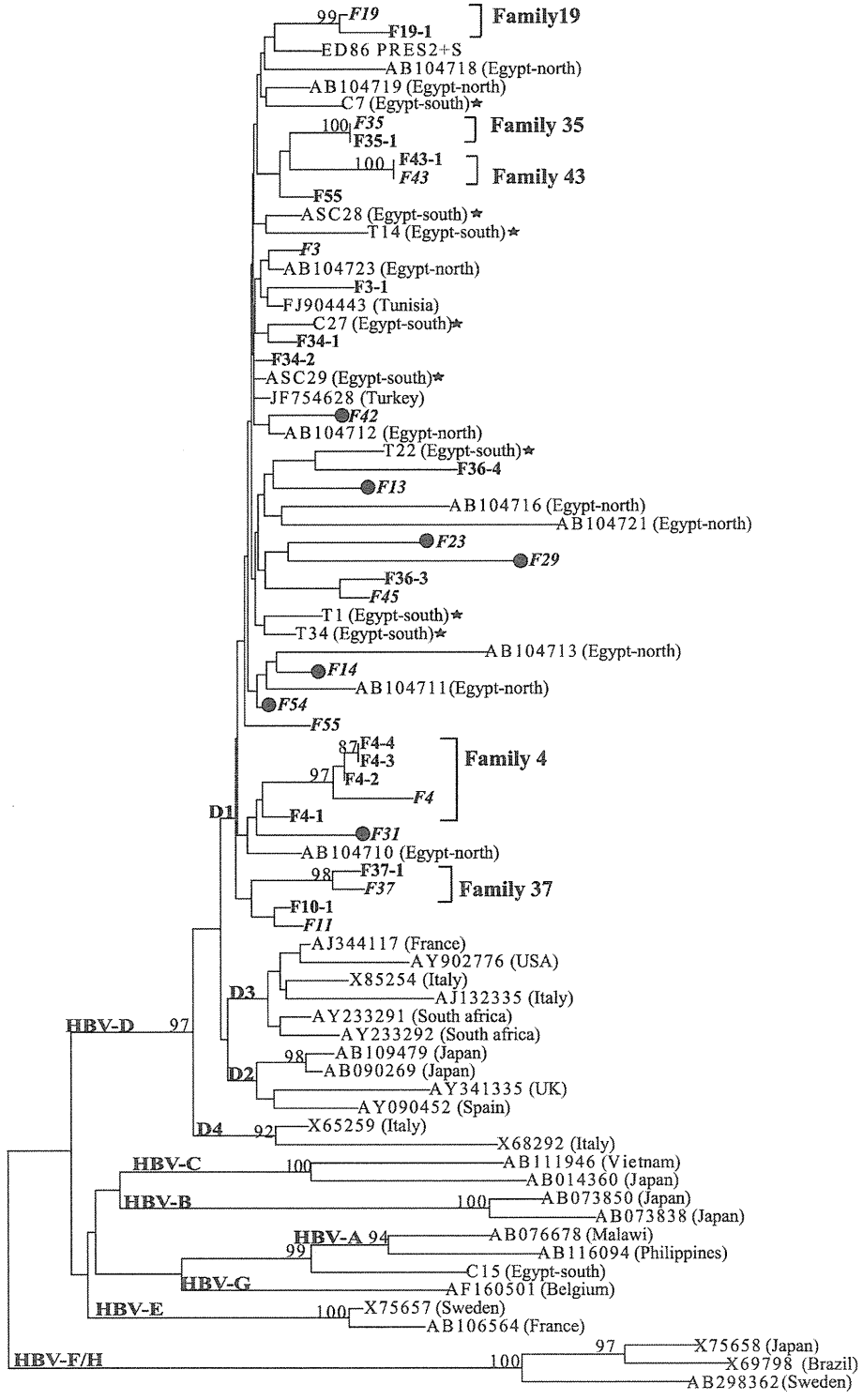

Fig. 3. Phylogenetic tree constructed by the nucleotide sequences of the partial PreS2 and S HBV genomic region. The phylogenetic tree is constructed by the neighbor joining method and significant bootstrap values (>75%) are indicated in the tree roots. HBV sequences isolated from index cases and family members are indicated in italic bold and bold fonts respectively. Reference sequences retrieved from the GenBank/EMBL/DDBJ are indicted in their accession numbers. Solid black rounds indicate sequences from index cases with family members negative for HBsAg. (★) Strains isolated from chronic hepatitis B carriers residing in Egypt south. The country origin of the reference sequences are indicated in brackets. HBV genotypes A–H are indicated in the cluster roots.

TABLE II. Comparison of Hepatitis B Serological Markers in Vaccinated Versus Unvaccinated Family Members Group

	Total (N = 230)	Vaccinated group (N = 142)	Unvaccinated group (N = 88)	*P*-value
Age[a]	20.6 ± 14.6	13.3 ± 10.4	32.5 ± 51.7	<0.0001
Gender (Male)[b]	96(41.7)	64 (45.1)	32 (36.4)	NS
Anti-HBc (+)[b]	53 (23)	20 (14.1)	33 (37.5)	<0.0001
HBsAg (+)[b]	28 (12.2)	15 (10.6)	13 (14.8)	NS
Anti-HBs (+)[b]	128 (55.7)	99 (69.8)	29(33)	<0.0001
HBV-DNA (+)[b]	14 (50)	8 (53.3)	6 (46.2)	NS

[a]Mean ± SD.
[b]N (%).

In the present study, 12.1% of the family members were infected with HBV. This incidence was much higher than that detected among the blood donors (1.4%) resident in the same area in Egypt (data not shown). Clustering of the HBV infection within the families has been described in nearby countries located within the same zone of the HBV endemicity but with different incidences; 30% in Turkey, 15.8% in Greece, and 11.9% in Iran [Alizadeh et al., 2005; Zervou et al., 2005; Ucmak et al., 2007]. An important risk factor was found to be implicated in acquiring the infection among the family was the presence of female infected with HBV. Furthermore, the higher incidence of HBsAg positive rate among the offspring of the females' index cases than that of males index cases illustrates clearly the role of the mother in the transmission of HBV. Similarly, Salkic et al. [2007] reported the same observation in his study from Bosnia [Salkic et al., 2007]. However, in Taiwan no significant difference was found in the HBsAg positivity among the offspring of the two groups, suggesting the importance of the paternal as well as the maternal transmission for the HBV intra-familial spread in Taiwan [Lin et al., 2005].

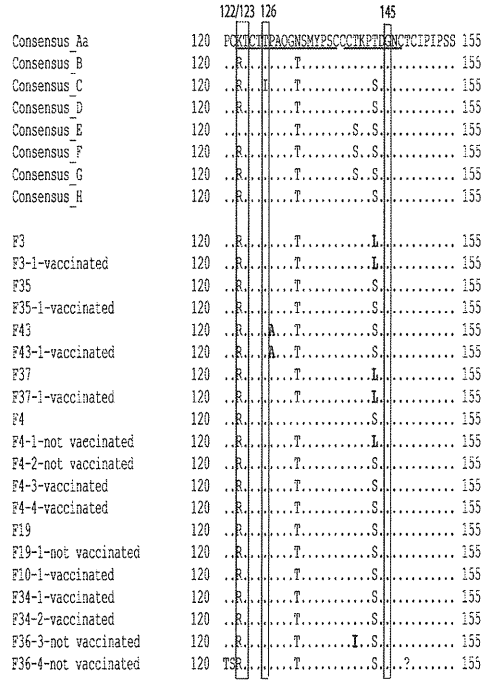

Fig. 4. The alignment of amino acid sequences of the HBV partial surface gene encompassing the "a" determinant region in the HBsAg positive family members. The upper eight sequences are consensus of the corresponding HBV genotypes Aa/A1, B, C, D, E, F, G, and H reference strain retrieved from DDBJ/GenBank database. Dots in alignment indicate identity of amino acids to the consensus sequence of genotype Aa/A1. First and second loop positions are underlined in the consensus sequence of the genotype Aa/A1 and positions of previously reported vaccine escape mutants are indicated in numbers and included in boxes.

Despite being a tedious and labor-intensive method, sequencing of the viral genomes isolated from different individuals, with the subsequent homology comparison and the phylogenetic analysis remains the golden approach for demonstrating the HBV transmission in a given population [Dumpis et al., 2001; Zampino et al., 2002; Tajiri et al., 2007].

The full length HBV sequence analysis is the gold standard for this purpose but remains a cost approach [Datta et al., 2007]. Highly variable HBV genomic region is recommended by some investigators to study the transmission event. Variability of the genomic region is affected by several factors one of which is the clinical characteristics of the studied cohort [Wu et al., 2005]. PreC/C region exhibit high variability in the cases of acute or fulminant hepatitis and thus analysis of this region is preferable for investigating the chain of recent/nosocomial fulminant cases [Bracho et al., 2006; Ozasa et al., 2006]. However, a high S gene variability is documented among the chronic hepatitis B carriers and their families, thus investigating the genotype, subgenotype, subtypes, and mutations by the sequence analysis of the S gene with further analysis by testing the constructed phylogenetic tree with the bootstrap resampling maximum-likelihood test, may provide enough confidence to prove the transmission event in the case of chronic HBV carriers [Thakur et al., 2003]. Hence, in the present study, the phylogenetic analysis of the HBV nucleotide sequences spanning the entire preS2 and S HBV genomic regions and isolated from chronic hepatitis B carriers which include index cases and their family members revealed the infection with HBV genotype D which coincides with the previous

data regarding the predominance of infection with HBV genotype D in Egypt [Saudy et al., 2003]. In addition, the phylogenetic analysis documented the presence of three different patterns of HBV genotype D transmission within the families in Egypt; maternal transmission (from mother to child as in the family 4), paternal transmission (from father to child as in family 35 and family 43) and spousal transmission (between spouses as in family 19 and family 37). This was different from the transmission pattern characteristics of genotype D in Uzbekistan where the horizontal transmission was the predominant route of infection with HBV genotype D within a family [Avazova et al., 2008].

The Data regarding the difference of transmission routes of HBV infection between different genotypes are controversial and scarce. Based on the findings that the patients infected with HBV genotype C may exhibit delayed HBeAg seroconversion decades later than the patients infected with other genotypes, Livingston et al. [2007] speculated that genotype C is the most responsible for the perinatal transmission and that the other genotypes (A, B, D, and F) are mainly transmitted horizontally [Livingston et al., 2007]. A recent study has shown a different data through exploring that both genotypes B and C can be transmitted by maternal and horizontal routes [Wen et al., 2011]. Whether different HBV genotypes have different transmission routes remains a question, which needs further global studies to clarify this interesting and important issue.

In an attempt to evaluate the influence of the universal vaccination on the intra-familial HBV infection, it was surprising to find a high prevalence rate of HBsAg among the vaccinated members with no significant difference when compared to the unvaccinated group. In an agreement with the present data, El Sherbini et al. [2006] reported the unchangeable prevalence of HBsAg among the vaccinated school children across a decade despite the significant decrease of the anti-HBc rate [El Sherbini et al., 2006]. The possible explanation for this vaccine failure is the acquiring of the HBV infection in the lag period between the birth and the time of receiving the first HBV vaccine dose at the age of 2 months. Supporting our explanation is the recent data coming from Taiwan where a different HBV infection prophylactic strategy is applied by administrating the first dose of the HBV vaccine at birth with the administration of the hepatitis B immunoglobulin to the infants born to the HBeAg positive mother within 24 hr after birth. The recent study has clearly demonstrated that the current HBV prophylactic strategy in Taiwan was capable of reducing the intra-familial HBV transmission and reducing the overall HBsAg positive rate among the infants [Mu et al., 2011]. In Japan, the extension of the active and passive immunization to the babies born to HBeAg negative mother had greatly reduced the HBsAg prevalence to 0.2% of blood donors younger than 19 years old [Noto et al., 2003; Matsuura et al., 2009]. The present study recommends the changing of the current HBV prophylactic policy in Egypt. It would be needed to provide the first dose of the HBV vaccine at birth together with screening for HBV infection markers prenatally and administration of the HBIG to the infants born from HBeAg-positive mothers. The documented role of the HBV spousal transmission in the present study by the phylogenetic analysis (Family 19 and Family 37), coincides with the recent data conducted in Egypt that the first sexual contact with an infected spouse was a significant risk factor for infection with HBV among females and may further emphasize the importance of the premarital screening for HBV in Egypt [Paez Jimenez et al., 2009]. Investigating the " a" determinant region of viral isolates retrieved from the vaccinated members infected with HBV provides no evidence of breakthrough infection by previously reported vaccine escape mutant virus [Carman et al., 1990].

In conclusion, the present study has clearly explored the role of the HBV intra-familial transmission and spread in north Eastern Egypt. Three patterns of HBV transmission were determined in the current cohort infected with HBV genotype D; maternal, paternal, and spousal. The present study recommends the change of the current prophylactic policy against the HBV infection in Egypt by including the first dose of HBV vaccine at birth, screening of pregnant women for HBsAg and the administration of HBIG to the infants born from HBeAg positive mothers within 24 hr after birth. Further studies are needed globally to determine the transmission patterns of different HBV genotypes and locally in different districts in Egypt to explore the impact of familial transmission in HBV infection in Egypt.

REFERENCES

Abdel-Wahab M, el-Enein AA, Abou-Zeid M, el-Fiky A, Abdallah T, Fawzy M, Fouad A, Sultan A, Fathy O, el-Ebidy G, elghawalby N, Ezzat F. 2000. Hepatocellular carcinoma in Mansoura-Egypt: Experience of 385 patients at a single center. Hepatogastroenterology 47:663–668.

Alizadeh AH, Ranjbar M, Ansari S, Alavian SM, Shalmani HM, Hekmat L, Zali MR. 2005. Intra-familial prevalence of hepatitis B virologic markers in HBsAg positive family members in Nahavand, Iran World J Gastroenterol 11:4857–4860.

Arthur RR, el-Sharkawy MS, Cope SE, Botros BA, Oun S, Morrill JC, Shope RE, Hibbs RG, Darwish MA, Imam IZ. 1993. Recurrence of Rift Valley fever in Egypt. Lancet 342:1149–1150.

Avazova D, Kurbanov F, Tanaka Y, Sugiyama M, Radchenko I, Ruziev D, Musabaev E, Mizokami M. 2008. Hepatitis B virus transmission pattern and vaccination efficiency in Uzbekistan. J Med Virol 80:217–224.

Bracho MA, Gosalbes MJ, Gonzalez F, Moya A, Gonzalez-Candelas F. 2006. Molecular epidemiology and evolution in an outbreak of fulminant hepatitis B virus. J Clin Microbiol 44:1288–1294.

Carman WF, Zanetti AR, Karayiannis P, Waters J, Manzillo G, Tanzi E, Zuckerman AJ, Thomas HC. 1990. Vaccine-induced escape mutant of hepatitis B virus. Lancet 336:325–329.

Chen DS. 1993. From hepatitis to hepatoma: Lessons from type B viral hepatitis. Science 262:369–370.

Custer B, Sullivan SD, Hazlet TK, Iloeje U, Veenstra DL, Kowdley KV. 2004. Global epidemiology of hepatitis B virus. J Clin Gastroenterol 38:S158–S168.

Datta S, Banerjee A, Chandra PK, Chakravarty R. 2007. Selecting a genetic region for molecular analysis of hepatitis B virus transmission. J Clin Microbiol 45:687; author reply 688.

Dumpis U, Holmes EC, Mendy M, Hill A, Thursz M, Hall A, Whittle H, Karayiannis P. 2001. Transmission of hepatitis B virus infection in Gambian families revealed by phylogenetic analysis. J Hepatol 35:99–104.

el Gohary A, Hassan A, Nooman Z, Lavanchy D, Mayerat X, el Ayat A, Fawaz N, Gobran F, Ahmed M, Kawano F, Ragheb M, Elkady A, Tanaka Y, Murakami S, Attia FM, Hassan AA, Hassan MF, Shedid MM, Abdel Reheem HB, Khan A, Mizokami M. 1995. High prevalence of hepatitis C virus among urban and rural population groups in Egypt. Acta Trop 59:155–161.

El Sherbini A, Mohsen SA, Seleem Z, Ghany AA, Moneib A, Abaza AH. 2006. Hepatitis B virus among schoolchildren in an endemic area in Egypt over a decade: Impact of hepatitis B vaccine. Am J Infect Control 34:600–602.

el-Zayadi A, Selim O, Rafik M, el-Haddad S. 1992. Prevalence of hepatitis C virus among non-A, non-B-related chronic liver disease in Egypt. J Hepatol 14:416–417.

el-Zayadi AR, Badran HM, Barakat EM, Attia Mel D, Shawky S, Mohamed MK, Selim O, Saeid A. 2005. Hepatocellular carcinoma in Egypt: A single center study over a decade. World J Gastroenterol 11:5193–5198.

Kao JH, Chen DS. 2002. Global control of hepatitis B virus infection. Lancet Infect Dis 2:395–403.

Lavanchy D. 2004. Hepatitis B virus epidemiology, disease burden, treatment, and current and emerging prevention and control measures. J Viral Hepat 11:97–107.

Lee WM. 1997. Hepatitis B virus infection. N Engl J Med 337:1733–1745.

Lin CL, Kao JH, Chen BF, Chen PJ, Lai MY, Chen DS. 2005. Application of hepatitis B virus genotyping and phylogenetic analysis in intrafamilial transmission of hepatitis B virus. Clin Infect Dis 41:1576–1581.

Livingston SE, Simonetti JP, Bulkow LR, Homan CE, Snowball MM, Cagle HH, Negus SE, McMahon BJ. 2007. Clearance of hepatitis B e antigen in patients with chronic hepatitis B and genotypes A, B, C, D, and F. Gastroenterology 133:1452–1457.

Matsuura K, Tanaka Y, Hige S, Yamada G, Murawaki Y, Komatsu M, Kuramitsu T, Kawata S, Tanaka E, Izumi N, Okuse C, Kakumu S, Okanoue T, Hino K, Hiasa Y, Sata M, Maeshiro T, Sugauchi F, Nojiri S, Joh T, Miyakawa Y, Mizokami M. 2009. Distribution of hepatitis B virus genotypes among patients with chronic infection in Japan shifting toward an increase of genotype A. J Clin Microbiol 47:1476–1483.

Milas J, Ropac D, Mulic R, Milas V, Valek I, Zoric I, Kozul K. 2000. Hepatitis B in the family. Eur J Epidemiol 16:203–208.

Miyakawa Y, Mizokami M. 2003. Classifying hepatitis B virus genotypes. Intervirology 46:329–338.

Mu SC, Wang GM, Jow GM, Chen BF. 2011. Impact of universal vaccination on intrafamilial transmission of hepatitis B virus. J Med Virol 83:783–790.

Norder H, Courouce AM, Magnius LO. 1994. Complete genomes, phylogenetic relatedness, and structural proteins of six strains of the hepatitis B virus, four of which represent two new genotypes. Virology 198:489–503.

Noto H, Terao T, Ryou S, Hirose Y, Yoshida T, Ookubo H, Mito H, Yoshizawa H. 2003. Combined passive and active immunoprophylaxis for preventing perinatal transmission of the hepatitis B virus carrier state in Shizuoka, Japan during 1980–1994. J Gastroenterol Hepatol 18:943–949.

Okamoto H, Tsuda F, Sakugawa H, Sastrosoewignjo RI, Imai M, Miyakawa Y, Mayumi M. 1988. Typing hepatitis B virus by homology in nucleotide sequence: Comparison of surface antigen subtypes. J Gen Virol 69:2575–2583.

Ozasa A, Tanaka Y, Orito E, Sugiyama M, Kang JH, Hige S, Kuramitsu T, Suzuki K, Tanaka E, Okada S, Tokita H, Asahina Y, Inoue K, Kakumu S, Okanoue T, Murawaki Y, Hino K, Onji M, Yatsuhashi H, Sakugawa H, Miyakawa Y, Ueda R, Mizokami M. 2006. Influence of genotypes and precore mutations on fulminant or chronic outcome of acute hepatitis B virus infection. Hepatology 44:326–334.

Paez Jimenez A, El-Din NS, El-Hoseiny M, El-Daly M, Abdel-Hamid M, El Aidi S, Sultan Y, El-Sayed N, Mohamed MK, Fontanet A. 2009. Community transmission of hepatitis B virus in Egypt: Results from a case–control study in Greater Cairo. Int J Epidemiol 38:757–765.

Poland GA, Jacobson RM. 2004. Clinical practice: Prevention of hepatitis B with the hepatitis B vaccine. N Engl J Med 351:2832–2838.

Salkic NN, Zildzic M, Muminhodzic K, Pavlovic-Calic N, Zerem E, Ahmetagic S, Mott-Divkovic S, Alibegovic E. 2007. Intrafamilial transmission of hepatitis B in Tuzla region of Bosnia and Herzegovina. Eur J Gastroenterol Hepatol 19:113–118.

Saudy N, Sugauchi F, Tanaka Y, Suzuki S, Aal AA, Zaid MA, Agha S, Mizokami M. 2003. Genotypes and phylogenetic characterization of hepatitis B and delta viruses in Egypt. J Med Virol 70: 529–536.

Schaefer S. 2005. Hepatitis B virus: Significance of genotypes. J Viral Hepat 12:111–124.

Seeger C, Mason WS. 2000. Hepatitis B virus biology. Microbiol Mol Biol Rev 64:51–68.

Shin IT, Tanaka Y, Tateno Y, Mizokami M. 2008. Development and public release of a comprehensive hepatitis virus database. Hepatol Res 38:234–243.

Stuyver L, De Gendt S, Van Geyt C, Zoulim F, Fried M, Schinazi RF, Rossau R. 2000. A new genotype of hepatitis B virus: Complete genome and phylogenetic relatedness. J Gen Virol 81: 67–74.

Sugauchi F, Mizokami M, Orito E, Ohno T, Kato H, Suzuki S, Kimura Y, Ueda R, Butterworth LA, Cooksley WG. 2001. A novel variant genotype C of hepatitis B virus identified in isolates from Australian Aborigines: Complete genome sequence and phylogenetic relatedness. J Gen Virol 82:883–892.

Sugiyama M, Tanaka Y, Kato T, Orito E, Ito K, Acharya SK, Gish RG, Kramvis A, Shimada T, Izumi N, Kaito M, Miyakawa Y, Mizokami M. 2006. Influence of hepatitis B virus genotypes on the intra- and extracellular expression of viral DNA and antigens. Hepatology 44:915–924.

Tajiri H, Tanaka Y, Kagimoto S, Murakami J, Tokuhara D, Mizokami M. 2007. Molecular evidence of father-to-child transmission of hepatitis B virus. J Med Virol 79:922–926.

Thakur V, Guptan RC, Malhotra V, Basir SF, Sarin SK. 2002. Prevalence of hepatitis B infection within family contacts of chronic liver disease patients – Does HBeAg positivity really matter? J Assoc Physicians India 50:1386–1394.

Thakur V, Kazim SN, Guptan RC, Malhotra V, Sarin SK. 2003. Molecular epidemiology and transmission of hepatitis B virus in close family contacts of HBV-related chronic liver disease patients. J Med Virol 70:520–528.

Thompson JD, Higgins DG, Gibson TJ. 1994. CLUSTAL W: Improving the sensitivity of progressive multiple sequence alignment through sequence weighting, position-specific gap penalties and weight matrix choice. Nucleic Acids Res 22:4673–4680.

Ucmak H, Faruk Kokoglu O, Celik M, Ergun UG. 2007. Intra-familial spread of hepatitis B virus infection in eastern Turkey. Epidemiol Infect 135:1338–1343.

Wen WH, Chen HL, Ni YH, Hsu HY, Kao JH, Hu FC, Chang MH. 2011. Secular trend of the viral genotype distribution in children with chronic hepatitis B virus infection after universal infant immunization. Hepatology 53:429–436.

Wu W, Chen Y, Ruan B, Li LJ. 2005. Gene heterogeneity of hepatitis B virus isolates from patients with severe hepatitis B. Hepatobiliary Pancreat Dis Int 4:530–534.

Zakaria S, Fouad R, Shaker O, Zaki S, Hashem A, El-Kamary SS, Esmat G, Zakaria S. 2007. Changing patterns of acute viral hepatitis at a major urban referral center in Egypt. Clin Infect Dis 44:e30–e36.

Zampino R, Lobello S, Chiaramonte M, Venturi-Pasini C, Dumpis U, Thursz M, Karayiannis P. 2002. Intra-familial transmission of hepatitis B virus in Italy: Phylogenetic sequence analysis and amino-acid variation of the core gene. J Hepatol 36:248–253.

Zekri AR, Hafez MM, Mohamed NI, Hassan ZK, El-Sayed MH, Khaled MM, Mansour T. 2007. Hepatitis B virus (HBV) genotypes in Egyptian pediatric cancer patients with acute and chronic active HBV infection. Virol J 4:74.

Zervou EK, Gatselis NK, Xanthi E, Ziciadis K, Georgiadou SP, Dalekos GN. 2005. Intrafamilial spread of hepatitis B virus infection in Greece. Eur J Gastroenterol Hepatol 17:911–915.

Zuckerman AJ. 1997. Prevention of primary liver cancer by immunization. N Engl J Med 336:1906–1907.

Journal of Controlled Release 163 (2012) 267–276

Contents lists available at SciVerse ScienceDirect

Journal of Controlled Release

journal homepage: www.elsevier.com/locate/jconrel

A pH-sensitive cationic lipid facilitates the delivery of liposomal siRNA and gene silencing activity *in vitro* and *in vivo*

Yusuke Sato [a], Hiroto Hatakeyama [a,b], Yu Sakurai [a], Mamoru Hyodo [a], Hidetaka Akita [a,b], Hideyoshi Harashima [a,b,*]

[a] *Faculty of Pharmaceutical Sciences, Hokkaido University, Sapporo, Hokkaido, Japan*
[b] *Core Research for Educational Science and Technology (CREST), Japan Science and Technology Agency, Kawaguchi, Saitama, Japan*

ARTICLE INFO

Article history:
Received 22 May 2012
Accepted 13 September 2012
Available online 20 September 2012

Keywords:
Multifunctional envelope-type nano device (MEND)
siRNA delivery
pH-sensitive cationic lipid
Intracellular trafficking
Endosomal escape

ABSTRACT

Modification of liposomal siRNA carriers with polyethylene glycol, *i.e.*, PEGylation, is a generally accepted strategy for achieving *in vivo* stability and delivery to tumor tissue. However, PEGylation significantly inhibits both cellular uptake and the endosomal escape process of the carriers. In a previous study, we reported on the development of a multifunctional envelope-type nano device (MEND) for siRNA delivery and peptide-based functional devices for overcoming the limitations and succeeded in the efficient delivery of siRNA to tumors. In this study, we synthesized a pH-sensitive cationic lipid, YSK05, to overcome the limitations. The YSK05-MEND had a higher ability for endosomal escape than other MENDs containing conventional cationic lipids. The PEGylated YSK05-MEND induced efficient gene silencing and overcame the limitations followed by optimization of the lipid composition. Furthermore, the intratumoral administration of the YSK05-MEND resulted in a more efficient gene silencing compared with MENDs containing conventional cationic lipids. Collectively, these data confirm that YSK05 facilitates the endosomal escape of the MEND and thereby enhances the efficacy of siRNA delivery into cytosol and gene silencing.

1. Introduction

RNA interference (RNAi) can be used as novel therapeutic procedure through the specific *in vivo* silencing of therapeutically relevant target genes [1,2]. Small interfering RNA (siRNA) duplexes are promising candidates for therapeutic molecules that might be capable of achieving the sequence-specific inhibition of objective genes such as for oncogenes in carcinomas. The most significant issue for bringing out the potency of siRNAs is an efficient delivery system, because the high molecular weight (~13 kDa) and negative charge of siRNA molecules are serious limitations to the passive diffusion across the plasma membrane of most cells and susceptibility to enzymatic degradation in an *in vivo* environment [3,4]. Therefore, although delivering siRNA without a carrier may be possible in some cases [5,6], systemic delivery to various tissues, including tumors, demands a carrier to stabilize and transport siRNA to the target cells. Moreover, a carrier system is required, which can allow siRNA to avoid endosomal/lysosomal degradation and to be localized in the cytoplasm, where the RNAi machinery is located. Thus, a number of attempts to develop various nano carrier systems have been reported [7–12]. We also recently reported on the development of a unique siRNA delivery system, described as a multifunctional envelope-type nano device (MEND) [13,14].

It is generally accepted that prolonging the circulation time of a nano carrier will facilitate tumoral accumulation *via* the enhanced permeability and retention (EPR) effect [15]. Sterically stabilization of a lipid based nano carrier by poly(ethyleneglycol) (PEG) is the most popular method and is widely used to enhance circulation time by reducing nonspecific interaction between positively charged nano carriers and negatively charged serum components, leading to severe aggregation and rapid clearance from circulation by the reticuloendothelial system [16]. However, it is well-known that PEGylation leads to a severe decline of cellular uptake *via* endocytosis and the endosomal escape process of nano carriers, which results in the loss of efficacy for

Abbreviations: cDNA, Complementary DNA; CHE, Cholesteryl hexadecyl ether; Chol, Cholesterol; DMEM, Dulbecco's modified Eagle medium; DMG, Dimyristoyl-*sn*-glycerol; DSG, Distearoyl-*sn*-glycerol; DODAP, 1,2-Dioleoyl-3-dimethylammonium propane; DOPC, 1,2-Dioleoyl-*sn*-glycero-3-phosphatidylcholine; DOPE, 1,2-Dioleoyl-*sn*-glycero-3-phosphoethanolamine; DOTAP, 1,2-Dioleoyl-3-trimethylammonium propane; DSPC, 1,2-Distearoyl-*sn*-glycero-3-phosphatidylcholine; EPR, Enhanced permeability and retention; FBS, Fatal bovine albumin; LF2k, Lipofectamine 2000; LNPs, Lipid nanoparticles; MEND, Multifunctional envelope-type nano device; MMPs, Matrix metalloproteases; mRNA, Messenger RNA; PBS, Phosphate buffered saline; PCR, Polymerase chain reaction; PEG, Polyethyleneglycol; PLK1, Polo-like kinase 1; POPE, 1-Palmitoyl-2-oleoyl-*sn*-glycero-3-phosphoethanolamine; RACE, Rapid amplification of cDNA ends; RBC, Red blood cell; RISC, RNA-induced silencing complex; RNAi, RNA interference; siRNA, Short interference RNA; SNALP, Stable nucleic acid lipid nanoparticles; SOPC, 1-Stearoyl-2-oleoyl-*sn*-glycero-3-phosphatidylcholine; TNS, 6-(p-Toluidino)-2-naphthalenesulfonic acid.

* Corresponding author at: Faculty of Pharmaceutical Science, Hokkaido University, Sapporo, Hokkaido 060-0812, Japan. Tel.: +81 11 706 3919; fax: +81 11 706 4879.
E-mail address: harasima@pharm.hokudai.ac.jp (H. Harashima).

0168-3659/$ – see front matter © 2012 Elsevier B.V. All rights reserved.
http://dx.doi.org/10.1016/j.jconrel.2012.09.009

delivering siRNA into the cytoplasm [17,18]. In other words, PEGylation improves the pharmacokinetics but decreases the intracellular trafficking of the nanocarrier, a situation that we refer to as the 'PEG-dilemma' [19].

To resolve the PEG-dilemma, many groups have attempted to use functional devices, such as a cleavable PEG-lipid that is affected by an acidic or reducing condition [20,21]. We previously reported on the production of a functional PEG-lipid, PPD, that is affected by matrix metalloproteinases (MMPs), which are secreted by various tumor cells and succeeded in silencing marker gene expression in tumor tissue by the systemic administration of PPD modified MEND [22,23]. In addition, we reported that GALA, a pH-sensitive fusogenic peptide, modified MEND which could be applied to an *in vivo* intratumoral injection model and shGALA, a new shorter version of GALA, to improve the pharmacokinetics of the MEND, which was modified to achieve gene silencing in tumor tissue followed by systemic administration [23–26]. As other strategy, Semple S.C. et al. [27] reported that the pharmacokinetics of the lipid nanoparticles (LNPs) with an ionizable aminolipid, which is largely neutral but changes to a cationic form under acidic conditions, was improved compared to that with a conventional cationic lipid. The LNPs system also succeeded in tumor specific reporter gene expression, and gene silencing in orthotopic and subcutaneous tumors [28,29].

In the present study, we report on the development of a new pH-sensitive cationic lipid, YSK05, for improving the efficient intracellular trafficking and consequently the gene silencing activity of a MEND both *in vitro* and *in vivo* instead of peptide-based functional devices (PPD, GALA and shGALA). Our results suggest that by the suitable manipulation of intracellular trafficking, the successful delivery of siRNA can be achieved, both *in vitro* and *in vivo*.

2. Materials and methods

2.1. Materials

Anti-luciferase siRNA (sense: 5′-CCG UCG UAU UCG UGA GCA AdTdT-3′; antisense: 5′-UUG CUC ACG AAU ACG ACG GdTdT-3′) was purchased from Sigma (Ishikari, Japan). Anti-PLK1 siRNA (sense: 5′-AGA uCA CCC uCC UUA AAu AUU-3′; antisense: 5′-UAU UUA AGG AGG GUG AuC UUU-3′, 2′-OMe-modified nucleotides are in lowercase.) and Cy5-labeled anti-luciferase siRNA (sense: 5′-Cy5-GCG CUG CUG GUG CCA ACC CdTdT-3′; antisense: 5′-GGG UUG GCA CCA GCA GCA GCC CdTdT-3′) were purchased from Hokkaido System Science Co., Ltd. (Sapporo, Japan). Protamine was purchased from Calbiochem (San Diego, CA, USA). 1,2-Dioleoyl-3-trimethylammonium propane (DOTAP), 1,2-dioleolyl-3-dimethylammonium propane (DODAP), 1,2-dioleoyl-*sn*-glycero-3-phosphoethanolamine (DOPE), 1-stearoyl-2-oleyl-*sn*-glycero-3-phosphatidylcholine (SOPC), 1,2-dioleyl-*sn*-3-phosphatidylcholine (DOPC) and cholesterol were purchased from Avanti Polar Lipid (Alabaster, AL, USA). 1-Palmitoyl-2-oleoyl-*sn*-glycero-3-phosphoethanolamine (POPE), 1,2-distearoyl-*sn*-3-phosphatidylcholine (DSPC), 1,2-dimyristoyl-*sn*-glycerol, methoxyethyleneglycol 2000 ether (PEG-DMG), 1,2-distearoyl-*sn*-glycerol, and methoxyethyleneglycol 2000 ether (PEG-DSG) were purchased from NOF Corporation (Tokyo, Japan). ^{3}H-labeled cholesteryl hexadecyl ether (^{3}H-CHE) was purchased from PerkinElmer Life Science (Tokyo, Japan). 6-(p-Toluidino)-2-naphthalenesulfonic acid (TNS) was purchased from Wako Chemicals (Osaka, Japan). RiboGreen was purchased from Molecular Probes (Eugene, OR, USA). Lipofectamine 2000 (LF2k) and TRIZOL reagent were purchased from Invitrogen (Carlsbad, CA, USA). Dual-Luciferase Reporter Assay Reagent was purchased from Promega Corporation (Madison, WI, USA). HeLa human cervical carcinoma cells were purchased from RIKEN Cell Bank (Tsukuba, Japan). OS-RC-2 human renal cell carcinoma cells were kindly provided by K. Hida (Hokkaido University, Sapporo, Hokkaido, Japan).

2.2. Experimental animals

Male ICR mice and BALB/cAjcl nude mice were purchased from Japan SLC (Shizuoka, Japan) and CLEA (Tokyo, Japan), respectively. The experimental protocols were reviewed and approved by the Hokkaido University Animal Care Committee in accordance with the guidelines for the care and use of laboratory animals.

2.3. MEND formulations

All MENDs were prepared using a cationic lipid, a phospholipid, cholesterol and PEG-DMG using a *t*-BuOH dilution procedure. The initial MENDs had a component molar ratio of 30/40/30/3 (DOTAP, DODAP or YSK05/DOPE/cholesterol/PEG-DMG) and optimized YSK05 MEND had 50/25/25/3 (YSK05/POPE/cholesterol/PEG-DMG). PEG-DMG was used to stabilize the lipid membrane during the formulation process and for preservation. Typically, 1.5 mM lipids were dissolved in 90% *t*-BuOH solution. siRNA was complexed with protamine at a nitrogen/phosphate ratio of 1.1 in 1 mM citrate buffer (pH 4.5) and was titrated slowly to lipid solution under vigorous mixing to avoid low local concentration of *t*-BuOH and diluted quickly with citrate buffer to final concentration of <20% *t*-BuOH. Ultrafiltration was performed to remove *t*-BuOH, replacing external buffer with phosphate buffered saline (PBS, pH 7.4) and concentrating the MENDs. To incorporate PEG-DSG, the MENDs were incubated at 45 °C for 45 min with PEG-DSG at 5.0 mol% total lipid under 10 v/v% ethanol conditions. Again, ultrafiltration was performed against PBS to remove EtOH and for concentration. An empty MEND with the same lipid composition was prepared by a similar procedure, with the exception that an equivalent volume of 1 mM citrate buffer was titrated to the lipid solution instead of siRNA/protamine complex. Radiolabeled MENDs were prepared by adding a trace amount of ^{3}H-CHE to the lipid-*t*-BuOH solution prior to mixing with the siRNA/protamine complex. The average diameter and zeta-potential of MENDs were determined using a Zetasizer Nano ZS ZEN3600 (Malvern Instruments, Worcestershire, UK).

2.4. RiboGreen assay

To determine siRNA encapsulation efficiency and its concentration, RiboGreen fluorescence assay was performed. MENDs were diluted in 10 mM HEPES buffer at pH 7.4 containing 20 μg/mL dextran sulfate and RiboGreen in the presence or absence of 0.1 w/v% Triton X-100. Fluorescence was measured by Varioskan Flash (Thermo Scientific) with $\lambda_{ex} = 500$ nm, $\lambda_{em} = 525$ nm. siRNA concentration was calculated from siRNA standard curve. siRNA encapsulation efficiency was calculated by comparing siRNA concentration in the presence and absence of Triton X-100.

2.5. TNS assay

Thirty μM of MEND lipid and 6 μM of TNS were mixed in 200 μL of 20 mM citrate buffer, 20 mM sodium phosphate buffer or 20 mM Tris–HCl buffer, containing 130 mM NaCl, at a pH ranging from 3.0 to 9.0. Fluorescence was measured by a Varioskan Flash set up with $\lambda_{ex} = 321$ nm, $\lambda_{em} = 447$ nm at 37 °C. The pKa values were measured as the pH giving rise to half-maximal fluorescent intensity.

2.6. Stability of MENDs in mouse serum

Fresh mouse serum was collected from a male ICR mouse and mixed with free siRNA, a mixture of siRNA/protamine complex and the empty MEND, and MEND formulating siRNA followed by incubation at 37 °C for various periods. For disruption of the lipid bilayer of the MEND, 0.05 w/v% Triton X-100 was added to the incubation mixture. At selected time points, aliquots were frozen at −80 °C to stop siRNA degradation. Afterward, the samples were thawed at r.t. and

siRNA was immediately extracted with a phenol–chloroform–isoamylalcohol mixture. The aqueous phase, containing the siRNA, was run on 20% polyacrylamide gels. After 2 h of electrophoresis at 150 V, siRNA was stained and visualized with 1 μg/mL of ethidium bromide.

2.7. Cell culture and in vitro luciferase gene silencing

HeLa cells stably expressing Firefly and Renilla luciferase (HeLa-dluc) were cultured in cell-culture dishes (Corning) containing DMEM supplemented with 10% FBS, penicillin (100 U/mL), streptomycin (100 mg/mL) and G418 (0.4 mg/mL) at 37 °C in 5% CO_2. For luciferase gene silencing, HeLa-dluc cells were seeded at a density of 5000 cells per well in 96-well plates in growth medium 24 h prior to transfection and incubated overnight at 37 °C in 5% CO_2 to allow cells to become attached. For transfection, media containing MENDs at the indicated doses of siRNA were added to cells after aspiration of the spent media. LF2k, as a control, was used according to the manufacturer's protocol. The MENDs were allowed to incubate with cells for 24 h prior to analysis for luciferase expression. To evaluate whether the gene silencing activities of the MENDs depend on endosomal acidification, MEND suspension in media containing various concentrations of chloroquine or NH_4Cl was added to the cells after aspiration of the spent media. The MENDs were incubated for 4 h with the cells, and new media were added after aspiration of the spent media and then further incubated for 20 h prior to analysis for luciferase expression. Firefly and Renilla luciferase activities were analyzed using the Dual-Glo assay (Promega) according to manufacturer's protocol. Luminescence was measured using a luminometer (Luminescencer-PSN, ATTO, Japan). For data analysis, Firefly luciferase activity was normalized by Renilla luciferase activity and treated samples were compared to untreated samples to determine degree of luciferase silencing.

2.8. Cellular uptake

Twenty-four hours prior to transfection, HeLa-dluc cells were seeded at a density of 1×10^5 cells per well in 6-well plates in growth medium and incubated overnight at 37 °C in 5% CO_2 to allow cell attachment. For transfection, media containing ^{3}H-labeled MENDs were transferred to the cells after aspiration of spent media. MENDs were allowed to incubate with the cells from 1 to 24 h. At selected time points, the cells were washed twice with PBS containing heparin (20 U/mL) and lysed with passive lysis buffer (Promega). Radioactivity was determined using a LSC-6100 (ALOKA) scintillation counter. The amount of cellular uptake was represented as the % of total transfected radioactivity.

2.9. Hemolysis assay

Fresh red blood cells (RBCs) were collected from an ICR mouse and suspended in PBS. The RBC suspension was mixed with each quantity of empty MEND, and incubated at 37 °C for 30 min. After the incubation, the absorbance at 545 nm of the supernatant was measured after centrifugation (4 °C, 400 g, 5 min). The samples incubated with 0.5 w/v% Triton X-100 as a positive control and without MENDs as a negative control were also measured. The %hemolysis was represented as the % of the absorbance of positive the control.

2.10. Assessment of intracellular trafficking of MEND-siRNA using confocal microscopy

Twenty-four hours prior to transfection, HeLa-dluc cells were seeded at a density of 1×10^5 cells per dish in a glass based dish in growth medium and incubated overnight at 37 °C in 5% CO_2 to allow cell attachment. For transfection, media containing 100 nM of Cy5-labeled siRNA formulated in optimized YSK05-MEND or DODAP-MEND were added to the cells and incubated for 1 h after aspiration of the spent media. The incubation was stopped by removing the media followed by washing the dishes three times with cold PBS. For the sample for the 6 hour time point, fresh media was then added and the cells were incubated at 37 °C for further 6 h and washed in cold PBS. After the washes, the cells were fixed with 4% paraformaldehyde (Wako Chemicals) for 10 min at room temperature. The cells were washed in PBS, then stained with nuclear marker Hoechst 33342 (Wako Chemicals) for 10 min to identify individual cells. After several washes, the cells were viewed using Nikon A1 (Nikon Co. Ltd., Tokyo, Japan) to assess the intracellular pattern of Cy5-labeled siRNA. Images were captured with ×60 objective following excitation with a 633 nm laser.

2.11. In vivo gene silencing activity of MENDs in tumor tissue

OS-RC-2 cells were cultured in cell culture dishes (Corning) containing RPMI1640 supplemented with 10% FBS, penicillin (100 U/mL) and streptomycin (100 mg/mL) at 37 °C in 5% CO_2. Tumor bearing mice were prepared by subcutaneous injection of male BALB/c nude mice with OS-RC-2 cells (1×10^6 cells/mouse). When the size of the tumor reached around 100 mm^3, MENDs were administrated to tumor tissue at a dose of 10 μg siRNA. At 24 h after administration, tumor tissues were collected, and approximately 30 mg of the tumor tissue was homogenized using PreCellys 24 (Bertin Technologies, France). The resulting tumor homogenates were centrifuged at 15,000 rpm for 10 min at 4 °C to obtain the supernatants. Total RNA (1 μg) was isolated with RNeasy (Qiagen) and reverse transcribed using a High Capacity RNA-to-cDNA kit (ABI) according to manufacturer's protocol. A quantitative PCR analysis was performed on 2 ng of cDNA using Fast SYBR Green Master Mix (ABI) and LightCycler 480 system II (Roche). All reactions were performed at a volume of 15 μL. The primers for human PLK1 were (forward) 5′-AAT AAA GGC TTG GAG AAC CC-3′ and (reverse) 5′-ACC TCA CCT GTC TCT CGA AC-3′ and for human GAPDH were (forward) 5′-CCT CTG ACT TCA ACA GCG AC-3′ and (reverse) 5′-CGT TGT CAT ACC AGG AAA TGA G-3′.

2.12. 5′ rapid amplification of cDNA ends-PCR (5′ RACE PCR)

Total RNA was isolated from *in vitro* cultured cell by lysis in TRIZOL. For *in vivo* tumor samples, approximately 30 mg of the tumor tissue was homogenized in 500 μL TRIZOL, then processed to isolate total RNA. Five μg of total RNA was heated to 65 °C for 5 min and snap-cooled to 4 °C prior to ligation. RNA ligation was performed at 37 °C for 1 h in 1× ligation buffer, T4 RNA ligase (TaKaRa, Japan) and 1.2 μg RNA adaptor (5′-NH_2-CGA CUG GAG CAC GAG GAC ACU GAC AUG GAC UGA AGG AGU AGA AA-3′). The samples were then purified by phenol–chloroform–isoamylalcohol extraction and ethanol precipitation. The RNA ligation product (10 μL) was reverse transcribed using SuperScript III (Invitrogen) and PLK1 gene specific primer (5′-GGA CAA GGC TGT AGA ACC CAC AC-3′). After heat denaturalization at 65 °C for 5 min followed by snap cooling at 4 °C, reverse transcription was carried out at 50 °C for 1 h followed by inactivation at 70 °C for 15 min and snap-cooling at 4 °C. 5′ RACE PCR was performed using forward primer (Ad1) in the RNA adaptor and reverse primer (Rev1) in the 3′ end of PLK1 mRNA. PCR primer sequences were Ad1 5′-CGA CTG GAG CAC GAG GAC ACT GA-3′ and Rev1 5′-GCT TGT CCA CCA TAG TGC GG-3′. PCR was performed using a 2720 Thermal Cycler (ABI) using touchdown PCR conditions of 94 °C for 2 min (1 cycle), 94 °C for 30 s and 72 °C for 40 s (5 cycles), 94 °C for 30 s and 70 °C for 40 s (5 cycles), 94 °C for 30 s and 66 °C for 30 s and 72 °C for 40 s (25 cycles), and 72 °C for 10 min (1 cycle). Nested PCR was then performed using the forward primer (Ad2) in the RNA adaptor 3′ to the Ad1 and reverse primer (Rev2) in the PLK1 mRNA 5′ to the Rev1. PCR primer sequences were Ad2 5′-GGA CAC TGA CAT GGA CTG AAG GAG TA-3′ and Rev2 5′-TCC TTG CAG CAG CCG TAC TC-3′. Nested PCR was performed using the same

instrument with PCR conditions of 94 °C for 2 min (1 cycle), 94 °C for 30 s and 64 °C for 30 s and 72 °C for 40 s (20 cycles), and 72 °C for 10 min (1 cycle). PCR products were run on a 2% TBE agarose gel and stained and visualized with 1 μg/mL of ethidium bromide.

3. Results

3.1. Synthesis of YSK05

DOTAP and DODAP are commercially available cationic lipids for transfection. The former is a quaternary ammonium derivative, resulting in cationic properties that are independent of the pH environment (Fig. 1). In contrast, the latter has a structure similar to DOTAP except that it contains a tertiary amine instead of a quaternary ammonium group resulting in pH-sensitive properties and becomes cationic at an acidic pH and is almost neutral at physiological pH. It is known that unsaturated carbon chains cause the formation of cone shaped molecules which promote transfection efficiency by facilitating the process of endosomal escape. Attempts to design new lipid structures based on this well known knowledge and in consideration of the ease of synthesis resulted in the successful synthesis of YSK05 as described. YSK05, newly synthesized in this laboratory, also contains one tertiary amine which confers pH-sensitive properties, and long, unsaturated carbon chains for emphasizing a cone shaped structure (Fig. 1). The yield was 62% (Supplementary materials).

3.2. Characteristics of the prepared MENDs

To prepare small and uniform particles and efficiently encapsulate siRNA reproducibly, MENDs were formulated by a *t*-BuOH dilution process as described. Particle size, zeta-potential, siRNA encapsulation and apparent pKa were assessed and the data are shown in Table 1. Diameters of all of the MENDs were approximately the same (115–125 nm). Three MENDs containing the pH-sensitive cationic lipid were approximately neutral at a pH of 7.4 and showed a high siRNA encapsulation efficiency (>90%), on the other hand, only the DOTAP-MEND showed high cationic properties and a somewhat low encapsulation efficiency. The apparent pKa of MENDs containing the pH-sensitive cationic lipid was measured using the fluorescent probe, TNS. It was observed that the apparent pKa of YSK05-MEND was around 6.5, while that of DODAP-MEND was lower than 6.0 (Supplementary Fig. 1).

Table 1
Physical properties of MENDs.

	MENDs			
	DOTAP	DODAP	YSK05	Optimized YSK05
Diameter (nm)	125 ± 1	119 ± 6	115 ± 5	116 ± 5
Polydispersity	0.16 ± 0.02	0.14 ± 0.02	0.15 ± 0.01	0.09 ± 0.02
Zeta potential (mV)	+20.3 ± 1.8	−1.6 ± 1.3	+4.5 ± 2.1	+4.5 ± 2.1
siRNA encapsulation (%)	67 ± 16	90 ± 5	90 ± 6	93 ± 4
Apparent pKa	–	5.8	6.6	6.4

Particle diameter, polydispersity and zeta-potential were measured using a Malvern Zetasizer. Percentage of siRNA encapsulation was determined by RiboGreen fluorescence assay to measure the amount of siRNA relative to total siRNA present. Apparent pKa value was determined by TNS fluorescence assay as a pH giving rise to half-maximal fluorescent intensity. Data points are expressed as the mean ± SD (n = 3).

Particle diameter, polydispersity and zeta-potential were measured using a Malvern Zetasizer. Percentage of siRNA encapsulation was determined by RiboGreen fluorescence assay to measure the amount of siRNA relative to total siRNA present. Apparent pKa value was determined by TNS fluorescence assay as a pH giving rise to half-maximal fluorescent intensity. Data points are expressed as the mean ± SD (n = 3).

3.3. YSK05-MEND indicates highest membrane disrupt potency and gene silencing activity in vitro

The ability of MENDs containing each cationic lipid to induce gene silencing in HeLa-dluc cells was evaluated. It was found that YSK05-MEND indicated higher gene silencing activity than DOTAP-MEND and its IC_{50} (that is, the dose to achieve 50% gene silencing) was around 30 nM, while DODAP-MEND failed to induce clear gene silencing (Fig. 2a). The amount of cellular uptake of each formulation was next measured with MENDs with incorporated ^{3}H-labeled CHE (Fig. 2b). The cellular uptake of the MEND containing DOTAP, pH-insensitive cationic lipid, was highest, while that of MENDs containing each pH-sensitive cationic lipid, almost neutral at physiological pH, was relatively low and similar to one another. The ability of MENDs to induce membrane disruption with RBC membranes was evaluated to judge the potency for escape

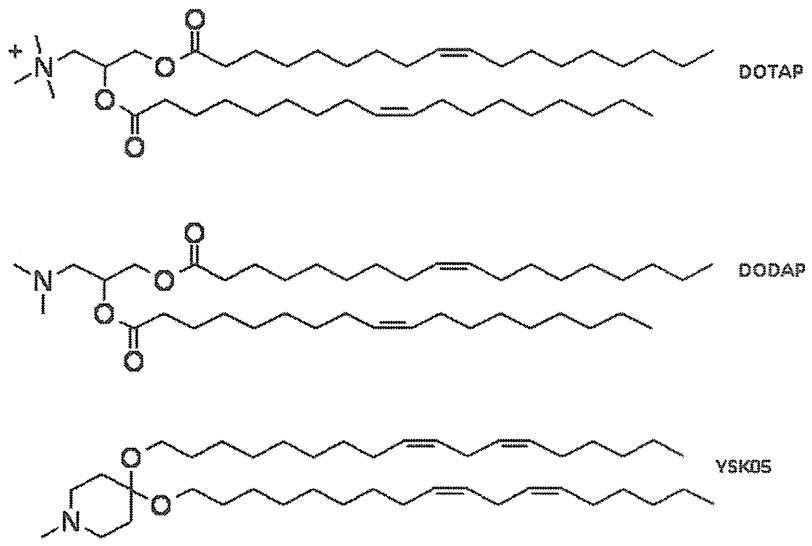

Fig. 1. Chemical structures of cationic lipids incorporated into MENDs. DOTAP and DODAP are conventional and available cationic lipids which have quaternary ammonium, indicating cationic without depending on pH, and tertiary amine, indicating cationic at acidic pH and neutral at physiological pH, respectively. YSK05 is a cationic lipid that contains a tertiary amine group for pH-sensitivity.

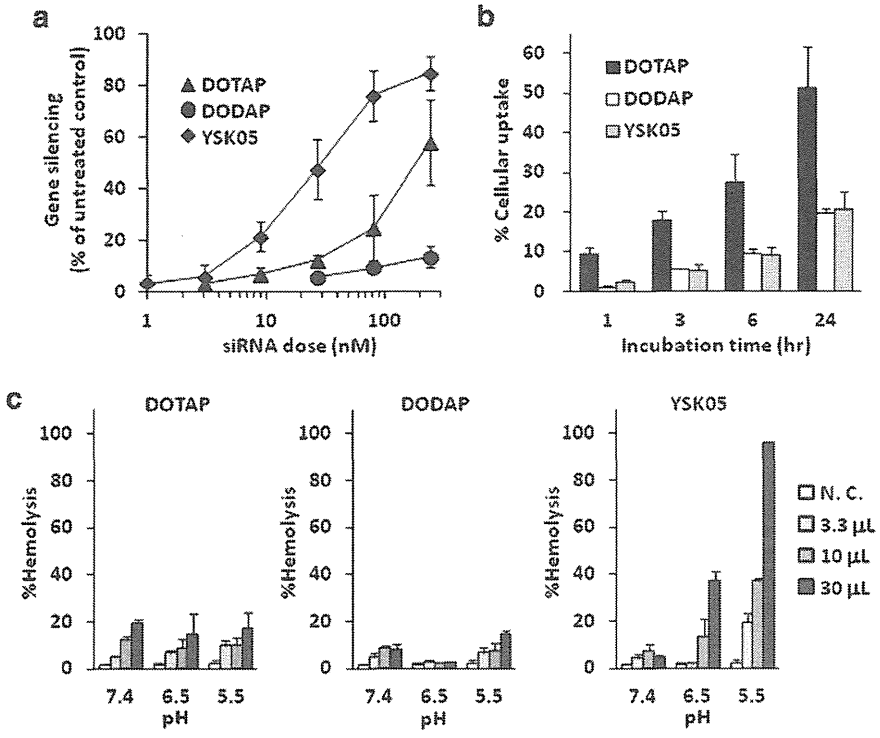

Fig. 2. Comparison of MENDs containing each cationic lipid *in vitro*. (a) MEND mediated gene silencing *in vitro*. HeLa-dluc cells were treated with MENDs containing anti-luciferase siRNA for 24 h. (b) Cellular uptake of MEND. HeLa-dluc cells were treated with MENDs containing ^{3}H-labeled CHE for various times. The cells were washed to remove unincorporated MENDs prior to measurement of ^{3}H-CHE. (c) MEND mediated hemolysis *in vitro*. RBC suspension was mixed with empty DOTAP- (left), DODAP- (center) or YSK05- (right) MEND and incubated for 30 min at 37 °C. The absorbance due to hemoglobin was measured after removal of intact RBCs by centrifugation. Data points are represented as the mean ± SD (n = 3). N.C.; negative control, P.C.; positive control.

from the endosomal compartment *via* membrane fusion. As shown in Fig. 2c, it was observed that YSK05-MEND induced membrane disruption depending on the dose of MENDs and decline of pH, while other two MENDs induced only minor membrane disruption even at low pH.

3.4. Optimization of YSK05-MEND lipid composition

To enhance the potency of the YSK05-MEND, the influence of phospholipid on gene silencing activity was evaluated. We used three phosphatidylcholine and two phosphatidylethanolamine derivatives as candidate phospholipids. It was observed that the YSK05-MEND containing any phosphatidylcholine (PC) failed to induce high gene silencing activity, while phosphatidylethanolamine (PE) succeeded (Supplementary Fig. 2). Additionally, we found that YSK05-MEND containing POPE had a higher gene silencing potency than DOPE and the highest stability in mouse serum of all tested phospholipids. Moreover, we found the optimal ratio of lipid combination through the screening of the lipid composition of YSK05-MEND, containing YSK05, POPE and cholesterol. The resulted YSK05-MEND, represented as optimized YSK05-MEND (YSK05/POPE/cholesterol = 50/25/25), indicated similar physical properties compared to the unoptimized one (Table 1) and the IC_{50} of 2 nM, approximately 15 times lower than the unoptimized one (Fig. 3a). The cellular uptake of optimized YSK05-MEND was almost similar to that for the unoptimized one (Fig. 3b), while the hemolytic activity of the former was significantly higher than the latter (Fig. 3c). Namely, it was revealed that the escalation of gene silencing activity through the optimization resulted from the escalation of the endosomal escape ability but not cellular uptake. We also evaluated the durability of gene silencing of the optimized YSK05-MEND (Supplementary Fig. 4). The findings indicate that the durability of gene silencing was dependent on the dose of siRNA, and the gene silencing rate decreased to 50% or below on day 4 at a dose of 10 nM siRNA and on day 7 at a dose of 100 nM siRNA.

3.5. YSK05-MEND internalizes via endocytosis and escapes depending on endosomal acidification

To further investigate the intracellular fate of siRNA formulated in the YSK05-MEND, Cy5-labeled siRNA was encapsulated in DODAP-MENDs and optimized in YSK05-MENDs and observed in HeLa-dluc cells using confocal microscope (Fig. 4a and Supplementary Fig. 3). Most of the Cy5 fluorescence of both formulations exhibited a punctuate pattern at the 0 hour time point, suggesting that both formulations were internalized into cells *via* endocytosis (Fig. 4a, upper). However, at the 6 hour time point, a formulation dependent difference was observed in the intracellular distribution pattern of Cy5-labeled siRNA in HeLa-dluc cells (Fig. 4a, lower). Cy5-labeled siRNA formulated in DODAP-MENDs exhibited a punctuate pattern at the 6 hour time point, the same as that of the 0 hour time point. In contrast, most Cy5-labeled siRNA formulated in optimized YSK05-MENDs exhibited a diffuse distribution at the 6 hour time point. This result suggests that the optimized YSK05-MEND delivered siRNA into the cytoplasm by escaping lysosomal degradation following internalization *via* endocytosis. To confirm that the release of siRNA in the cytoplasm by the YSK05-MEND was dependent on endosomal acidification, the gene silencing activity of the optimized YSK05-MEND was evaluated in the presence of an inhibitor of endosomal acidification (Fig. 4b). Two low molecular weight drugs, chloroquine and ammonium chloride (NH_4Cl), were used for buffering acidic vesicles, resulting in the inhibition of lysosomal enzymes and possibly altering normal lysosomal trafficking. DOTAP-MEND was used as a control of pH-independent carrier. The gene silencing activity of DOTAP-MEND slightly increased depending on drug concentration,

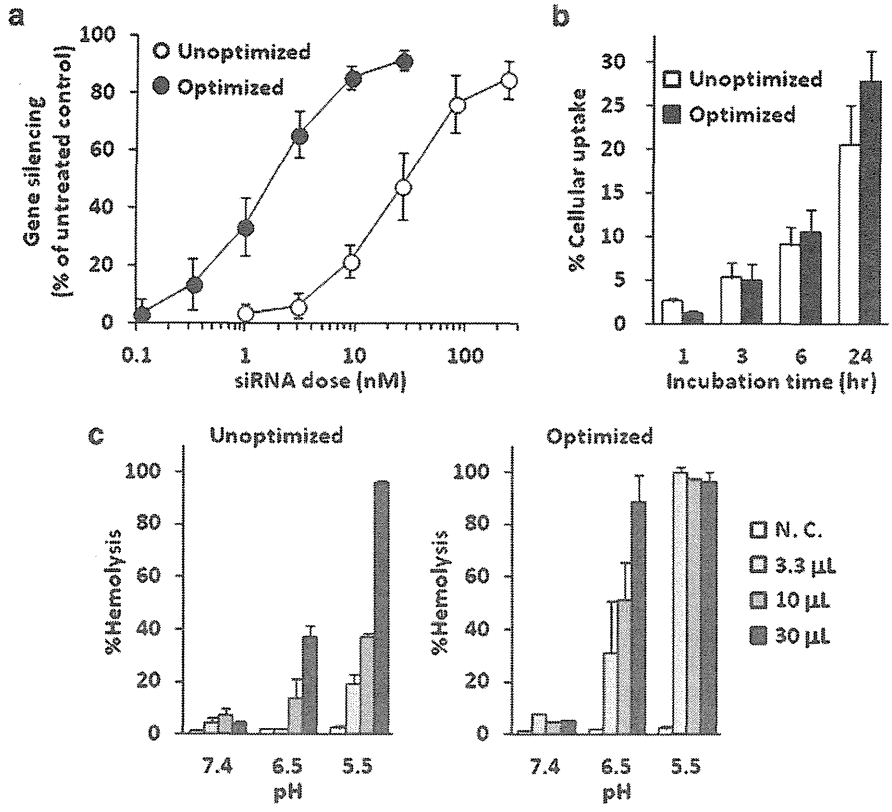

Fig. 3. Comparison of YSK05-MENDs before and after optimization of lipid composition. (a) MEND mediated gene silencing *in vitro*. HeLa-dluc cells were treated with MENDs containing anti-luciferase siRNA for 24 h (n = 3–6). (b) Cellular uptake of MEND. HeLa-dluc cells were treated with MENDs containing ^{3}H-labeled CHE for various times. The cells were washed to remove unincorporated MENDs prior to measurement of ^{3}H-CHE (n = 3). (c) MEND mediated hemolysis *in vitro*. RBC suspension was mixed with empty unoptimized (left) or optimized (right) YSK05-MEND and incubated for 30 min at 37 °C. The absorbance from hemoglobin was measured after removal of intact RBCs by centrifugation (n = 3). Data points are represented as the mean ± SD. N.C.; negative control, P.C.; positive control.

while that of YSK05-MEND was significantly suppressed by both drugs. From these results, it was confirmed that optimized YSK05-MEND was taken up into cells *via* endocytosis and escaped from endosome significantly depending on endosomal acidification followed by inducing gene silencing.

3.6. PEGylated optimized YSK05-MEND induces gene silencing both in vitro and in vivo

The incorporation of PEG-DSG into optimized YSK05-MENDs was carried out to provide stability under an *in vivo* environment. It is known that PEG lipid with a long acyl chain, such as PEG-DSG, is retained strongly by a lipid membrane while PEG lipid with short acyl chain, such as PEG-DMG, is dissociated more readily from a membrane [28]. After the incorporation of PEG-DSG, the stability of the optimized YSK05-MEND in serum was significantly increased, as expected (Supplementary Fig. 7). Next, to evaluate gene silencing activity in tumor tissue, anti-polo-like kinase 1 (PLK1) siRNA (siPLK1) formulated in PEG-DSG modified MENDs with each having different lipid compositions was topically administrated on OS-RC-2 subcutaneous tumors. Although MENDs containing DOTAP and DODAP failed to induce gene silencing, the unoptimized and optimized YSK05-MENDs succeeded approximately 30% and 50% gene silencing was found, respectively (Fig. 5c). To confirm that gene silencing was clearly the result of RNAi, we detected the RNAi-specific PLK1 mRNA cleavage product by the 5′ RACE PCR method. Active PLK1 mRNA cleavage was detected only after administration of siPLK1 formulated in optimized YSK05-MEND but not the non-treatment control or the anti-luciferase siRNA (siGL4) control, clearly demonstrating that a sequence specific RNAi occurred in tumor tissues (Fig. 5d).

4. Discussion

There are several obstacles to the delivery of siRNA. These include its safe delivery to the target cell population, internalization into the cells and escape from the endosomal compartment for protection from lysosomal degradation and localization in the cytoplasm, where siRNAs are located and function. PEGylation enhances the stability and half-life of nano carriers in blood circulation by avoiding recognition and clearance by phagocytic cells of the reticuloendothelial system and is widely used in *in vivo* applications of nano carriers. As the conventional MEND was composed of a cationic lipid, such as DOTAP, it was necessary to modify the conventional cationic MEND with high amounts of PEG lipids to suppress non-specific electrostatic interactions with internal components, such as negatively charged proteins [22,23,26]. However, it is also known that PEGylation results in a significant loss of gene silencing efficiency. We previously showed that the two intracellular processes, cellular uptake and endosomal escape, are suppressed by PEGylation. The outer PEG layer sterically hinders interaction between a carrier and cell surface membrane, and results in a decrease in cellular uptake *via* endocytosis. After uptake, the PEG layer similarly inhibits endosomal escape *via* membrane fusion between the carrier membrane and the endosomal membrane. In order to solve this problem, it is necessary to remove or reduce the level of the PEG moiety. Strategies for overcoming the PEG-dilemma are outlined below. The first is acceleration of steps that are inhibited, such as cellular uptake and endosomal escape, by introducing functional devices into highly PEG-modified carriers. As shown previously, more than 10 mol% of PEG is necessary to achieve sufficient blood circulation in the case of a cationic DOTAP-MEND [22]. Therefore, the highly

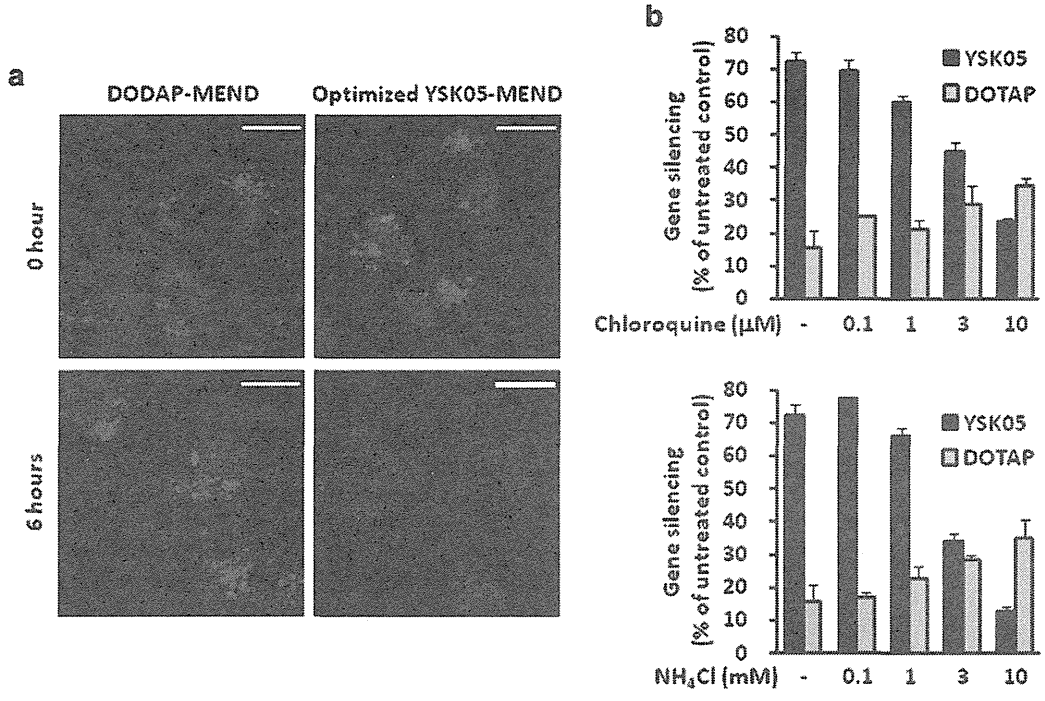

Fig. 4. Confirming the endosomal escape of optimized YSK05-MEND. (a) The intracellular pattern and distribution of siRNA. HeLa-dluc cells were treated with Cy5-labeled siRNA formulated in DODAP- (left) or optimized YSK05- (right) MEND at a dose of 100 nM siRNA for 1 h. Unincorporated MENDs were washed out and siRNA distribution was visualized after 0 h (upper) or 6 h (lower) using a confocal microscopy. Scale bars indicate 20 μm. Full-size pictures are presented in Supplementary Fig. 3. (b) MEND mediated gene silencing in the presence of the chemicals buffering endosome. HeLa-dluc cells were treated with anti-luciferase siRNA formulated in DOTAP-MEND (150 nM) and optimized in YSK05-MEND (27 nM) in the presence of chloroquine (upper) or NH_4Cl (lower) for 4 h. The cells were further incubated for 20 h after medium change. Data points are represented as the mean ± SD (n = 3).

PEGylated DOTAP-MEND was modified with enzymatically cleavable PEG [23] or a shorter version the GALA peptide [26] to achieve both sufficient blood circulation and efficient silencing activity. The second approach is decreasing the level of the PEG moiety by introducing charge changeable devices. Conner, Yatvin, and Huang [30] proposed the concept of pH-sensitive liposomes, which release encapsulated drugs following an acid treatment. Judge AD and colleagues [31] prepared stable nucleic acid lipid particles (SNALP) and succeeded in achieving gene silencing in tumor tissue after the systemic administration of low amounts of PEG lipid used in the modification process. SNALP is composed of an ionizable amino lipid and it was reported that the chemical structure of the ionizable amino lipid has a significant influence on the intracellular fate of SNALP [32,33]. In this study, we synthesized a new pH-sensitive cationic lipid, YSK05, for the second purpose.

YSK05-MEND induced higher gene silencing activity than other MENDs containing each conventional cationic lipid, DOTAP and DODAP, a pH-insensitive and a pH-sensitive cationic lipid, respectively (Fig. 2). Despite its comparable cellular uptake, the YSK05-MEND showed a significantly higher gene silencing activity than DODAP-MEND. There are two reasons for this, as described below. One reason is that the YSK05-MEND with an apparent pKa of around 6.6 can rapidly become a cationic species in response to endosomal acidification and thus avoid lysosomal degradation, while the DODAP-MEND with an apparent pKa<6.0 cannot accomplish this, at least not rapidly (Table 1). The other reason is that YSK05-MEND has a considerably higher hemolytic activity than the DODAP-MEND, indicating that YSK05-MEND can more easily escape from endosomes *via* membrane fusion (Fig. 2c). It was verified, using confocal microscopy, that YSK05-MEND escapes from endosomes followed by releasing siRNA into the cytosol (Fig. 4a). Also, the YSK05-MEND indicated higher gene silencing activity than DOTAP-MEND in spite of the fact that the amount of cellular uptake of the former was lower than that of the latter (Fig. 2a and c). This result also can be explained from the observation that the YSK05-MEND has a significantly higher potency for membrane fusion than the DOTAP-MEND, as evidenced by hemolysis assay (Fig. 2c).

Additionally, the lipid composition significantly influenced the gene silencing activity of YSK05-MEND. YSK05-MENDs containing two phosphatidylethanolamines, DOPE and POPE, induced gene silencing at a dose of 9 nM, while the YSK05-MENDs containing all of the phosphatidylcholines failed (Supplementary Fig. 2b). The cause of this result might be the shape of the phospholipid molecules. It is generally accepted that phosphatidylethanolamine is classified as an inverted lipid capable of accelerating membrane fusion by inducing structural changes in the lipid membrane from a lamellar to an inverted hexagonal (H_{II}) phase, while phosphatidylcholine induced the formation of a cylindrical lipid capable of stabilizing a lamellar phase [34]. Although there is no direct evidence to show that the YSK05-MEND containing POPE has a higher gene silencing activity than DOPE, the excellent stability in serum of the former may account for this (Supplementary Fig. 2a). We next, carried out the screening of lipid composition of YSK05-MEND, containing YSK05, POPE and cholesterol, and represented the resulting MEND as the optimized YSK05-MEND. The physical parameters of the optimized YSK05-MEND were similar to the unoptimized preparation. The potential for endosomal escape but not for cellular uptake was enhanced through optimization of the lipid components and resulted in the escalation of gene silencing activity (Fig. 3). We then evaluated the durability of gene silencing of the optimized YSK05-MEND using HeLa-dluc cells. The durability of gene silencing was extended by increasing the dose of siRNA from 10 nM to 100 nM. This result would result from a situation where the excess siRNAs in the cytosol were incorporated into the RNA-induced silencing complex (RISC) one after another following the degradation of siRNAs incorporated into RISC. Although the durability of gene silencing is dependent on the cell division rate, the stability of siRNA and so on, the span and pattern were similar to those reported in our previous study [35].

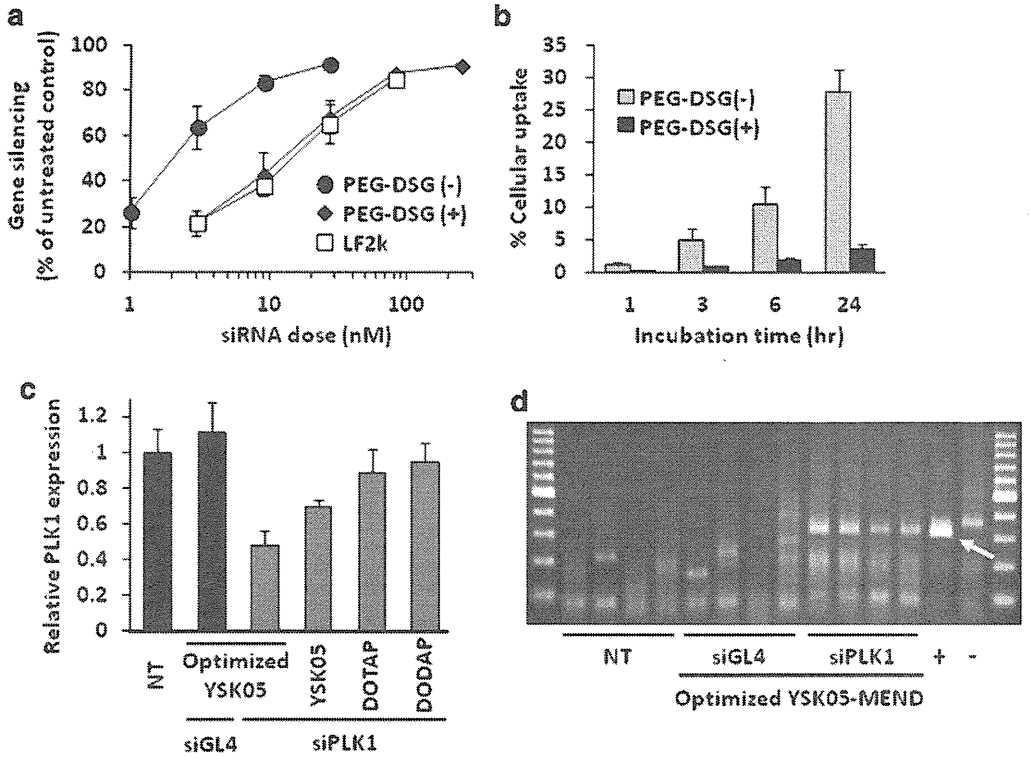

Fig. 5. Gene silencing activity of PEGylated optimized YSK05-MEND *in vitro* and *in vivo*. (a) MEND mediated gene silencing *in vitro*. HeLa-dluc cells were treated with MENDs and Lipofectamine 2000 (LF2k) incorporating anti-luciferase siRNA (siGL4) for 24 h (n = 3). (b) Cellular uptake. HeLa-dluc cells were treated with MENDs containing ^{3}H-labeled CHE for various times (n = 3). (c) MEND mediated gene silencing *in vivo*. OS-RC-2 tumor bearing mice were topically administrated with MENDs at a dose of 10 μg siPLK1 or siGL4 into tumors. After 24 h, the mice were euthanized and PLK1 gene expression was measured (n = 4). (d) 5′ RACE PCR analysis. RNAi specific PLK1 mRNA cleavage products were detected after 24 h topical administration of MENDs. Positive control from *in vitro* OS-RC-2 cell lysates treated with siPLK1 was indicated by plus sign and negative control was indicated by minus sign. RACE PCR detects the 5′ cleavage product of human PLK1 mRNA from tumors. Each lane represents different tumor tissues. The predicted 321-bp PLK1 product is indicated by an arrow. Data points are represented as the mean ± SD.

The result of confocal microscopy experiments confirmed that the optimized YSK05-MENDs were taken up *via* endocytosis and were able to release siRNA into the cytoplasm by endosomal escape after a 6 hour chase (Fig. 4a). In contrast, siRNA formulated in the DODAP-MEND showed a punctuate pattern even in the case of a 6 hour chase, indicating that the DODAP-MEND failed to escape from the endosomal compartments. This result corresponds to the failure of both gene silencing and hemolysis. To elucidate the dependence on pH decline for endosomal escape and further gene silencing of the YSK05-MEND, transfection in the presence of chloroquine and NH_4Cl was examined. Chloroquine and NH_4Cl are known to buffer the pH of endosomes and lysosomes and to improve the transfection efficiency of vectors which are unable to escape from the lysosomal trafficking pathway [36–39]. The gene silencing activity of DOTAP-MEND, a pH-insensitive carrier, gradually increased depending on the concentration of each compound, indicating that the endosomal escape efficacy of the DOTAP-MEND was increased by avoiding trafficking to degradative lysosomes. In contrast, the gene silencing activity of the optimized YSK05-MEND dramatically decreased, indicating that the endosomal escape process of the YSK05-MEND strongly depends on the acidification of endosomes as we expected (Fig. 4b).

Finally, we evaluated the gene silencing activity of the MENDs in tumor tissue. In this study, we chose the amount of PEG modification as 5 mol% of the total lipid, because the blood circulation of DODAP-MEND with 3.5 or more mol% of PEG was saturated, indicating that a 5 mol% PEG modification is sufficient in terms of preventing nonspecific interactions between DODAP-MEND, a pH-sensitive cationic system, and serum components (Supplementary Fig. 5). Actually, an attempt to induce gene silencing in OS-RC-2 subcutaneous tumor tissue by the intratumoral administration of optimized YSK05-MEND without incorporated PEG-DSG resulted in failure (data not shown). Although the reason for this is not clear, there are two possibilities. One possibility is that the stability of the optimized YSK05-MEND is too low to tolerate the *in vivo* environment. Another possibility is that the optimized YSK05-MEND was taken up by other cells in the tumor tissue, such as tumor associated macrophages, rather than tumor cells. Therefore, the surface of the MEND would have been shielded by the incorporation of PEG-DSG, increasing its physical stability and reducing non-specific cellular uptake. In an *in vitro* examination, the cellular uptake of the optimized YSK05-MEND with 5 mol% of incorporated PEG-DSG was severely reduced (Fig. 5a). This indicates that 5 mol% PEG modification is sufficient to prevent nonspecific interaction between the optimized YSK05-MEND and biomembranes at physiological pH. However, the gene silencing activity of the optimized YSK05-MEND with incorporated PEG-DSG was similar to that for LF2k, a commonly used transfection reagent (Fig. 5b), indicating that it escaped efficiently from endosomes. This result can be explained as follows. DOTAP-MEND, a cationic system, could be shielded by the 5 mol% PEG and more than 10 mol% PEG was necessary for shielding its surface sufficiently (Supplementary Fig. 5), indicating that 5 mol% PEG was not sufficient to shield the highly cationic surface of the MEND. Once the optimized YSK05-MEND is internalized *via* endocytosis, YSK05 (50 mol% of the total lipid) was immediately protonated in the acidified interior of the endosome. Therefore, only 5 mol% of PEG could not sufficiently prevent the interaction between the protonated (cationic) YSK05 of the MEND lipid bilayer and anionic lipids of the endosomal membrane, resulting in efficient endosomal escape. This suggests that YSK05 is sufficiently potent to permit it to overcome the PEG dilemma, compared to the use of PPD and GALA, as we had previously reported [21,22,24]. PEG-DSG incorporated MENDs containing various lipid compositions were topically

administrated on OS-RC-2 subcutaneous tumors and the gene silencing activity of each MEND was evaluated *in vivo*. Only the MEND containing YSK05 was able to induce gene silencing, indicating that YSK05 is also able to overcome the PEG dilemma *in vivo* (Fig. 5c). Furthermore, it was revealed that the PEGylation of the YSK05-MEND was necessary to induce gene silencing in tumor tissues, because PEGylation resulted in increasing the stability of the YSK05-MEND or changing the intratumoral trafficking of the YSK05-MEND. The result for 5′ RACE PCR suggests that the PLK1 gene silencing in tumor tissue surely results from a sequence specific RNAi mechanism (Fig. 5d). It is well-known that the suppression of PLK1 function or gene expression leads to apoptosis or the suppression of cell proliferation in most cancer cell lines. Given this fact, we evaluated PLK1 gene silencing and cytotoxicity on both OS-RC-2 cells and HeLa-dluc cells *in vitro* (Supplementary Fig. 7). The findings revealed that gene silencing by the optimized YSK05-MEND was induced more easily in OS-RC-2 cells than in HeLa-dluc cells (Supplementary Fig. 7a). However, cytotoxicity as the result of PLK1 silencing was not observed on OS-RC-2 cells, but was clearly observed in HeLa-dluc cells (Supplementary Fig. 7b, c). These findings, therefore, suggest that PLK1 gene silencing on OS-RC-2 subcutaneous tumor tissue by the topical administration of optimized YSK05-MEND would fail to induce an antitumor effect. To obtain an antitumor effect, it will be necessary to examine other target genes that are capable of inducing apoptosis or suppressing the cell proliferation of OS-RC-2 cells through its gene silencing.

5. Conclusion

The results of the present study indicate that the new pH-sensitive cationic lipid YSK05 improves the intracellular trafficking of non-viral vectors. In an *in vitro* study, the gene silencing efficiency of YSK05-MEND was significantly greater than that of DOTAP- and DODAP-MENDs. It was confirmed that YSK05-MEND efficiently escaped from endosomes and the process was strongly dependent on endosomal acidification. Furthermore, the PEG-DSG incorporated optimized YSK05-MEND showed a gene silencing activity that was similar to LF2k, suggesting that YSK05 overcame the suppression of endosomal escape by PEGylation. In the *in vivo* study, the optimized YSK05-MEND indicated most efficient gene silencing of all MENDs and RNAi mediated gene silencing was confirmed by the detection of sequence specific mRNA cleavage products using the 5′ RACE PCR method. Collectively, YSK05 effectively enhances siRNA delivery both *in vitro* and *in vivo*.

Acknowledgments

This study was supported in part by a Grant-in-Aid for Young Scientists (B) from the Japan Society for the Promotion of Science (JSPS), and a Grant-in-Aid for Scientific Research on Innovative Areas "Nanomedicine Molecular Science" (No. 2306) from Ministry of Education, Culture, Sports, Science, and Technology (MEXT) of Japan, and the Special Education and Research Expenses of the Ministry of Education, Culture, Sports, Science and Technology (MEXT) of Japan, and by a Grant for Industrial Technology Research from New Energy and Industrial Technology Development Organization (NEDO). The authors also wish to thank Dr. Milton S. Feather for his helpful advice in writing the English manuscript.

Appendix A. Supplementary data

Supplementary data to this article can be found online at http://dx.doi.org/10.1016/j.jconrel.2012.09.009.

References

[1] D.H. Kim, J.J. Rossi, Strategies for silencing human disease using RNA interference, Nat. Rev. Genet. 8 (2007) 173–184.
[2] A. Fougerolles, H.P. Vornlocher, J. Maraganore, J. Lieberman, Interfering with disease: a progress report on siRNA-based therapeutics, Nat. Rev. Drug Discov. 6 (2007) 443–453.
[3] J.M. Vargason, G. Szittya, J. Burgyan, T.M. Hall, Size selective recognition of siRNA by an RNA silencing suppressor, Cell 115 (2003) 799–811.
[4] A.D. Judge, V. Sood, J.R. Shaw, D. Fang, K. McClintock, I. MacLachlan, Sequence-dependent stimulation of the mammalian innate immune response by synthetic siRNA, Nat. Biotechnol. 23 (2005) 457–462.
[5] M.E. Kleinman, K. Yamada, A. Takeda, V. Chandrasekaran, M. Nozaki, J.Z. Baffi, R.J. Albuguergue, S. Yamasaki, M. Itaya, Y. Pan, B. Appukuttan, D. Gibbs, Z. Yang, K. Kariko, B.K. Ambati, T.A. Wilgus, L.A. DiPietro, E. Sakurai, K. Zhang, J.R. Smith, E.W. Taylor, J. Ambati, Sequence- and target-independent angiogenesis suppression by siRNA via TLR3, Nature 452 (2008) 591–597.
[6] V. Bitko, A. Musiyenko, O. Shulyayeva, S. Barik, Inhibition of respiratory viruses by nasally administered siRNA, Nat. Med. 11 (2005) 50–55.
[7] R.W. Malone, P.L. Felgner, I.M. Verma, Cationic liposome-mediated RNA transfection, Proc. Nat. Acad. Sci. U.S.A. 86 (1989) 6077–6081.
[8] A. Santel, M. Aleku, O. Keil, J. Endruschat, V. Esche, G. Fisch, S. Dames, K. Loffler, M. Fechtner, W. Arnold, K. Giese, A. Klippel, J. Kaufmann, A novel siRNA-lipoplex technology for RNA interference in the mouse vascular endothelium, Gene Ther. 13 (2006) 1222–1234.
[9] F. Takeshita, Y. Minakuchi, S. Nagahara, K. Honma, H. Sasaki, K. Hirai, T. Teratani, N. Namatame, Y. Yamamoto, K. Hanai, T. Kato, A. Sano, T. Ochiya, Efficient delivery of small interfering RNA to bone-metastatic tumors by using atelocollagen in vivo, Proc. Nat. Acad. Sci. U.S.A. 102 (2005) 12177–12182.
[10] D.B. Rozema, D.L. Lewis, D.H. Wakefield, S.C. Wong, J.J. Klein, P.L. Roesch, S.L. Bertin, T.W. Reppen, Q. Chu, A.V. Blokhin, J.E. Hagstrom, J.A. Wolff, Dynamic PolyConjugates for targeted in vivo delivery of siRNA to hepatocytes, Proc. Nat. Acad. Sci. U.S.A. 104 (2007) 12982–12987.
[11] T.S. Zimmerman, A.C. Lee, A. Akinc, B. Bramlage, D. Bumcrot, M.N. Fedoruk, J. Harborth, J.A. Heyes, L.B. Jeffs, M. John, A.D. Judge, K. Lam, K. McClintock, L.V. Nechev, L.R. Palmer, T. Racie, I. Rohl, S. Seiffert, S. Shanmugam, V. Sood, J. Soutschek, I. Toudjarska, A.J. Wheat, E. Yaworski, W. Zedalis, V. Koteliansky, M. Manoharan, H.P. Vornlocher, I. MacLachlan, RNAi-mediated gene silencing in non-human primates, Nature 441 (2006) 111–114.
[12] A. Akinc, A. Zumbuehl, M. Goldberg, E.S. Leshchiner, V. Busini, N. Hossain, S.A. Bacallado, D.N. Nguyen, J. Fuller, R. Alvarez, A. Borodovsky, T. Borland, R. Constien, A. de Fougerolles, J.R. Dorkin, K. Narayanannair Jayaprakash, M. Jayaraman, M. John, V. Koteliansky, M. Manoharan, L. Nechev, J. Qin, T. Racie, D. Raitcheva, K.G. Rajeev, D.W. Sah, J. Soutschek, I. Toudjarska, H.P. Vornlocher, T.S. Zimmermann, R. Langer, D.G. Anderson, A combinatorial library of lipid-like materials for delivery of RNAi therapeutics, Nat. Biotechnol. 26 (2008) 561–569.
[13] K. Kogure, R. Moriguchi, K. Sasaki, M. Ueno, S. Futaki, H. Harashima, Development of a non-viral multifunctional envelope-type nano device by a novel lipid film hydration method, J. Control. Release 98 (2004) 317–323.
[14] K. Kogure, H. Akita, H. Harashima, Multifunctional envelope-type nano device for non-viral gene delivery: concept and application of programmed packaging, J. Control. Release 122 (2007) 246–251.
[15] H. Maeda, J. Wu, T. Sawa, Y. Matsumura, K. Hori, Tumor vascular permeability and the EPR effect in macromolecular therapeutics: a review, J. Control. Release 65 (2000) 271–284.
[16] P. Tam, M. Monck, D. Lee, O. Ludkovski, E.C. Leng, K. Clow, H. Stark, P. Scherrer, R.W. Graham, P.R. Cullis, Stabilized plasmid–lipid particles for systemic gene therapy, Gene Ther. 7 (21) (2001) 1867–1874.
[17] S. Mishra, P. Webster, M.E. Davis, PEGylation significantly affects cellular uptake and intracellular trafficking of non-viral gene delivery particles, Eur. J. Cell Biol. 83 (2004) 97–111.
[18] K. Remaut, B. Lucas, K. Braeckmans, J. Demeester, S.C. De Smedt, Pegylation of liposomes favours the endosomal degradation of the delivered phosphodiester oligonucleotides, J. Control. Release 117 (2007) 256–266.
[19] H. Hatakeyama, H. Akita, H. Harashima, A multifunctional envelope type nano device (MEND) for gene delivery to tumours based on the EPR effect: a strategy for overcoming the PEG dilemma, Adv. Drug Deliv. Rev. 63 (2011) 152–160.
[20] J.S. Choi, J.A. MacKay, F.C. Szoka Jr., Low-pH-sensitive PEG-stabilized plasmid–lipid nanoparticles: preparation and characterization, Bioconjug Chem. 14 (2003) 20–29.
[21] R. Kuai, W. Yuan, Y. Qin, H. Chen, J. Tang, M. Yuan, Z. Zhang, Q. He, Efficient delivery of payload into tumor cells in a controlled manner by TAT and thiolytic cleavable PEG co-modified liposomes, Mol. Pharmacol. 7 (2010) 1816–1826.
[22] H. Hatakeyama, H. Akita, K. Kogure, M. Oishi, Y. Nagasaki, Y. Kihira, M. Ueno, H. Kobayashi, H. Kikuchi, H. Harashima, Development of a novel systemic gene delivery system for cancer therapy with a tumor-specific cleavable PEG-lipid, Gene Ther. 14 (2007) 68–77.
[23] H. Hatakeyama, H. Akita, E. Ito, Y. Hayashi, M. Oishi, Y. Nagasaki, R. Danev, K. Nagayama, N. Kaji, H. Kikuchi, Y. Baba, H. Harashima, Systemic delivery of siRNA to tumors using a lipid nanoparticle containing a tumor-specific cleavable PEG-lipid, Biomaterials 32 (2011) 4306–4316.
[24] H. Hatakeyama, E. Ito, H. Akita, M. Oishi, Y. Nagasaki, S. Futaki, H. Harashima, A pH-sensitive fusogenic peptide facilitates endosomal escape and greatly enhances the gene silencing of siRNA-containing nanoparticles in vitro and in vivo, J. Control. Release 139 (2009) 127–132.
[25] T. Kakudo, S. Chaki, S. Futaki, I. Nakase, K. Akaji, T. Kawakami, K. Maruyama, H. Kamiya, H. Harashima, Transferrin-modified liposomes equipped with a pH-sensitive fusogenic peptide: an artificial viral-like delivery system, Biochemistry 43 (2004) 5618–5628.
[26] Y. Sakurai, H. Hatakeyama, Y. Sato, H. Akita, K. Takayama, S. Kobayashi, S. Futaki, H. Harashima, Endosomal escape and the knockdown efficiency of liposomal-siRNA by the fusogenic peptide shGALA, Biomaterials 32 (2011) 5733–5742.